



## UWS Academic Portal

### **Technical evaluation of proton exchange membrane (PEM) fuel cell performance – A review of the effects of bipolar plates coating**

Wilberforce, Tabbi; Ijaodola, O.; Ogungbemi, Emmanuel; Khatib, F.N.; Leslie, T.; El-Hassan, Zaki; Thompson, J.; Olabi, A.G.

*Published in:*  
Renewable & Sustainable Energy Reviews

*DOI:*  
[10.1016/j.rser.2019.109286](https://doi.org/10.1016/j.rser.2019.109286)

Published: 31/10/2019

*Document Version*  
Peer reviewed version

[Link to publication on the UWS Academic Portal](#)

*Citation for published version (APA):*

Wilberforce, T., Ijaodola, O., Ogungbemi, E., Khatib, F. N., Leslie, T., El-Hassan, Z., Thompson, J., & Olabi, A. G. (2019). Technical evaluation of proton exchange membrane (PEM) fuel cell performance – A review of the effects of bipolar plates coating. *Renewable & Sustainable Energy Reviews*, 113, [109286].  
<https://doi.org/10.1016/j.rser.2019.109286>

#### **General rights**

Copyright and moral rights for the publications made accessible in the UWS Academic Portal are retained by the authors and/or other copyright owners and it is a condition of accessing publications that users recognise and abide by the legal requirements associated with these rights.

#### **Take down policy**

If you believe that this document breaches copyright please contact [pure@uws.ac.uk](mailto:pure@uws.ac.uk) providing details, and we will remove access to the work immediately and investigate your claim.

Technical Evaluation of Proton Exchange Membrane (PEM) fuel cell performance – A review  
Tabbi Wilberforce<sup>1\*</sup>, O. Ijaodola<sup>1</sup>, Emmanuel Ogungbemi<sup>1</sup>, F.N. Khatib<sup>1</sup>, T. Leslie<sup>1</sup>, Zaki El  
Hassan<sup>1</sup>, J. Thomposon<sup>1</sup>, A. G. Olabi<sup>2,3</sup>

1. Institute of Engineering and Energy Technologies, University of the West of Scotland, UK.
2. School of Engineering and Applied Science, Aston University, Aston Triangle, Birmingham B4 7ET, UK.
3. Dept. of Sustainable and Renewable Energy Engineering, University of Sharjah, P.O. Box 27272, Sharjah, UAE.

### Abstract

This investigation considered recent advancement made in material selection for bipolar plate (BP) for PEM fuel cell. The mechanical characteristics as well as the chemical characteristics of each material currently used for mass production of bipolar plate were also captured. The report delves more into the various techniques used in the coating of materials for BP. Several coating materials were also discussed. The impact of these coating materials on the efficiency of the fuel cell is also captured. Techniques adopted by researchers in coating applications with experimental justification are also captured in this report. The advantages and disadvantages of different surface treatment used in the development of bipolar plates is critically evaluated in this report. A conclusion was therefore deduced that for the cost of fuel cell to reduce to compete with other energy generation mediums, it is recommended that BPs are coated in order to curtail the effect of corrosion on the efficiency of the cell. Coating of BP improves corrosion resistance, interfacial contact resistance and corrosion current density. This report hence will serve as a manual for the fuel cell research community in their quest of improving the overall performance characteristics of fuel cells.

Key words: Bipolar plate, Interfacial contact resistance (ICR), Stainless steel, Polarization curve, Coating

## 1.0 Introduction

Energy is considered as the building block of life. The high reliance on fossil product for energy generation as well its environmental impact is the main contributing factor for the need to consider alternative forms of energy generation [1]. According to Yifei et al, 2016 [2] most fossil reserves are depleting gradually hence their sustainability cannot be guaranteed. Bizon and Phatiphat, 2018 [3] further argue that the prices of fossil commodities in recent times has been fluctuating making the cost of energy generation unstable. Places where some of these fossil products are extracted in their natural state have seen several unrests leading to the loss of properties and lives over the last few decades with Nigeria being a practical example. Scientists are considering other medium of energy generation due to the issues raised earlier. It must be noted that fossil products continue to dominate the energy industry till date [4-6]. Priya et al, 2018 [7] in their research concluded that renewable energy therefore remains the only alternative to fossil products as they are environmentally friendly. PEM fuel cells according to researchers are one of the types of renewable energy generation mediums that will give a better competition with fossil fuel [8-12]. This is mainly because they are environmentally friendly with no amount of carbon dioxide being released into the atmosphere during the energy generation process [13]. PEMFCs are energy converting device that transforms hydrogen and oxygen into electricity using membrane electrode assembly (MEA) as the platform where electrochemical reaction occurs. Platinum is often used as the catalyst to speed up the chemical reaction process [14]. The byproduct for the electrochemical reaction is hydrogen and heat. Fuel cells in general are highly efficient means of energy generation but PEM fuel cells have fast start up time and they are very robust. They also require less maintenance as there are no moving parts in their build up. The absence of no moving parts implies that the issue of wear and tear and excessive heat leading to huge losses is not a challenge in the usage of PEMFCs. All these are some merits in generating energy using PEMFCs. The main disadvantage in the usage of PEMFC is the cost of the device [15]. They are currently expensive compared to other type of energy generation. The cost of PEMFCs is often due to the weight of the device, the optimization processes on input parameters (flow rate, pressure, temperature etc.) as well as the modification of the components in the fuel cell. An important component in the cell is the BP. They operate as the medium where reactive substances enter the fuel cell and serves as the exit point for the byproduct of the cell [16-20].

The bipolar plate (flow plate) also functions as the collection point for all produced current from cell [21 – 25]. This means that a poorly designed bipolar plate will reduce the efficiency of the cell. Since most BPs in recent times are made up of metals, there is the need to consider coating the flow plate with suitable material to prevent corrosion but increase the electrical and thermal conductivity [26 – 30]. The work considers some specific research conducted on stainless steel and titanium. Due to their easy availability and cost, stainless steel is sometimes used in the production of BP. The ICR as well as  $I_{corr}$  of ferritic stainless steel was compared with SS316L. The order of the ICR was from 100 to 200m $\Omega$ cm<sup>2</sup> (SS444 > SS436 > SS441 > SS434 > SS316L > SS446). According to another investigation conducted by another researcher, the  $I_{corr}$  of SS316L, SS321 and SS347 are 0.26 x 10<sup>-4</sup>, 0.8 x 10<sup>-5</sup> and 1.58 x 10<sup>-5</sup> mAcm<sup>-2</sup> respectively. ICR of uncoated austenite stainless steel is normally greater than 100m $\Omega$ cm<sup>-2</sup> in anodic and cathodic region of PEMFC [18]. A conclusion can therefore be made that the bare stainless steel does not meet the US Department of Energy (DOE) criteria shown in Table 1.

Table 1: Specifications for material used for bipolar plates

Property	Unit	2017	2020
Weight	KgKW <sup>-1</sup>	<0.4	0.4
H <sub>2</sub> permeation rate	cm <sup>3</sup> (cm <sup>2</sup> s) <sup>-1</sup>	<1.3x10 <sup>-14</sup>	1.3x10 <sup>-14</sup>
Cost	\$KW <sup>-1</sup>	3	3
Corrosion at anode & cathode	$\mu$ Acm <sup>-2</sup>	<1	<1
Electrical conductivity	Scm <sup>-1</sup>	>100	>100
Flexural strength (ASTM D790-10)	MPa	>25	>25
Area specific resistance	$\Omega$ -cm <sup>2</sup>	0.02	0.01

The flow plates Corrosion characteristics for SS316L was also investigated by a group of researchers using varying Sulfuric acid (H<sub>2</sub>SO<sub>4</sub>) concentrations via electrochemical techniques. Increasing the concentrations of the H<sub>2</sub>SO<sub>4</sub> from 0 to 1 M according to their investigations made the  $I_{corr}$  increase appreciably from 0.84 to 640 mAcm<sup>-2</sup> and that of the interfacial contact resistance from 10 to 50m $\Omega$ cm<sup>-2</sup>. Their work further stated that the ICR between SS316L and carbon paper decreased as H<sub>2</sub>SO<sub>4</sub> concentrations increased. This condition changed when the passive film thickness increased. It also showed the need for the coating of SS316L using a thin conductive and protective layer.

This paper focuses on coated bipolar plates for proton exchange membrane (PEM) fuel cells applications. It involves investigation into the different materials used for coating bipolar plates, the process of stamping bipolar plates and various surface treatment adopted for the development of bipolar plates. Materials investigated include carbon, chromium, nitrogen, nickel, noble metals, non-ferrous alloys and aluminium. All these materials have potentials in have been highly considered by researchers in this field. Furthermore the process of stamping the bipolar plates for both bare and coated metals – hydroforming, is discussed. Surface treatments considered in this work include chemical approach, treatment via heat, ion implantation, spray coating and vapour deposition (VD).

### 1.1 Carbon coatings

The best coating suitable for stainless steel according to Feng et al [31] is carbon films. This conclusion was after performing potentiodynamic experiment and potentiostat experiment to determine rate of resistance to corrosion and the rate of corrosion for uncoated and coated material using carbon.

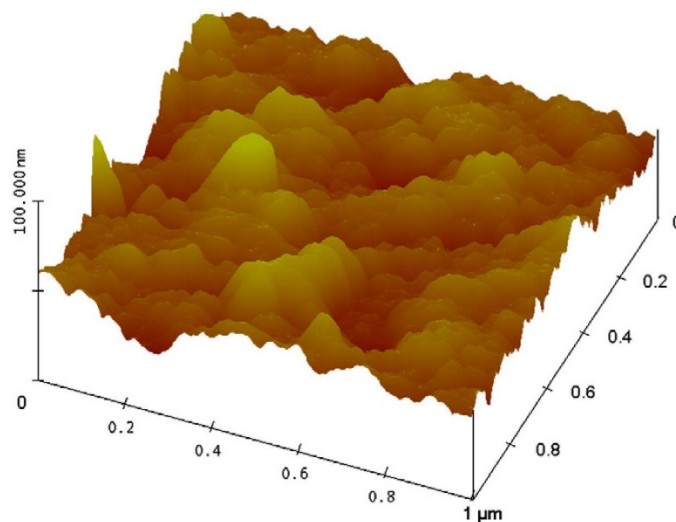


Fig. 1: Carbon film on SS316 (Authorization to reproduce obtained from ref. [32])

Feng et al [31] kept samples in a resin (epoxy) having an area of 10 x 10 mm<sup>2</sup>. By means of soldering, wire made of copper was fixed to the back of each material. Electrode system adopted

by the group was also made up of sheet of platinum. The platinum sheet functioned as counter electrode. The reference electrode was made of calomel electrode. The research group further performed electrochemical test in 0.5 M sulfuric acid to excite the hash PEM fuel cell conditions. Prior to electrochemical experiment, they recorded the open circuit potential against time for an hour to make sure the sample was electrically stable. The characteristics and how stable the uncoated and carbon coated materials behaved was also carried out using the potentiostatic test. The potentiostatic experiment was performed within 8.9 – 9hours at a potential of 0.6 V against the SCE but purged with air. The solution was then collected and inspected to ascertain the quantity of Iron, Chromium, Nickel and Molybdenum ions in the solution. The sample was then separated from the epoxy resin and all impurities eliminated using ethanol ultrasonically. The samples then went through scanning electron microscopy (SEM) prior and after the electrochemical experiment. This was to determine the processes as well as the impact of the corrosion on the bare and carbon coated Stainless Steel 316L. Using hydrophobic materials is one approach of curbing flooding in the cell stack as the H<sub>2</sub>O prevents easy movement of air or oxygen by blocking the flow channel or the pores in the GDL. Finally, data physics OCA20 contact angle system was utilized to determine the water contact angle on the carbon coated Stainless Steel 316L [31]. The ICR was also determined using the approach suggested by Davies and Brady according to Taherian, 2012 [32] as shown in Fig. 2 below.

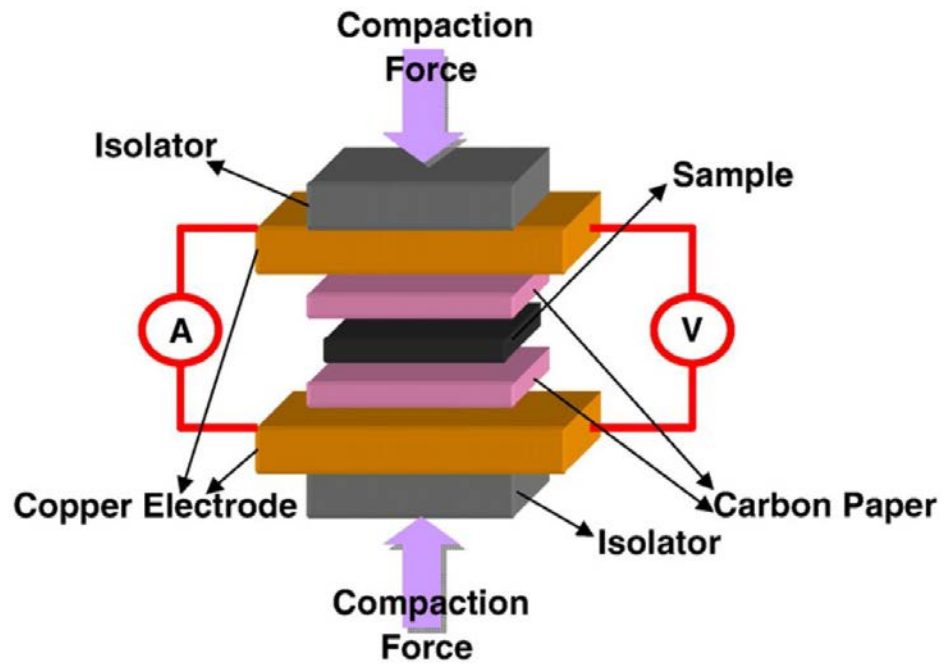


Fig. 2: Diagram for the set up used to determine the ICR (Authorization to reproduce obtained from ref. [34])

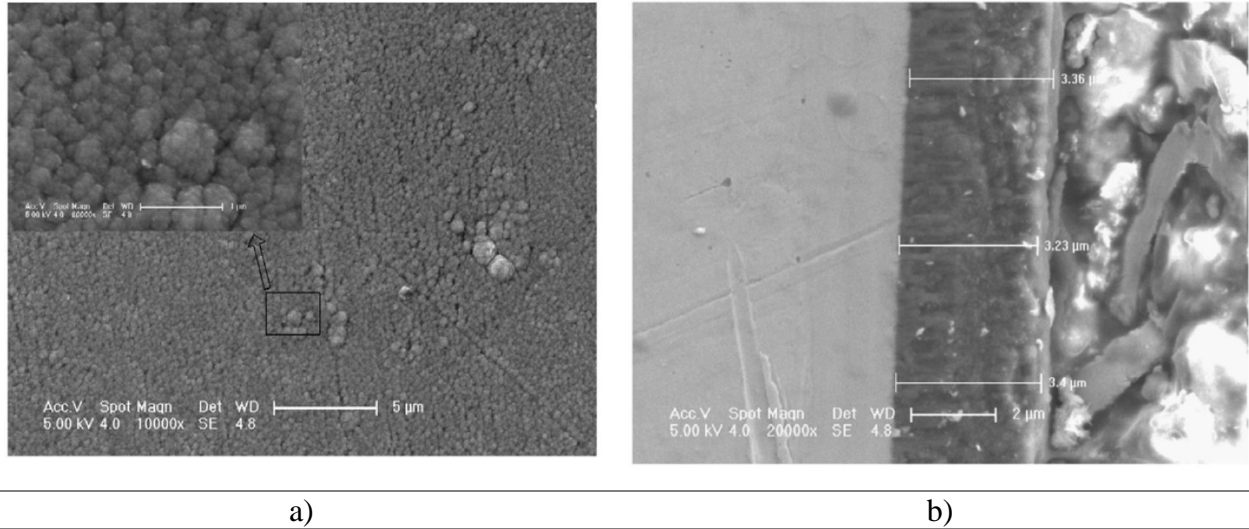


Fig. 3: Topology obtained from SEM a) cross sectional view b) thin film of carbon stainless steel 316L34 (Authorization to reproduce from [34])

Fig. 3 indicates the topology for thin film of carbon on stainless steel 316L material. From Fig. 3, it can be seen that the carbon film is made granules of carbon that are spherical, having diameters between 0.1 - 1μm. The carbon utilized also had a thickness of 3.3 μm as shown in Fig. 3b. The entire duration for the coating was 4hrs. Accumulation of the carbon spheres is what creates the carbon film which is very compact and dense as well. The carbon film serves as a layer that reduces the rate of corrosion on the substrate. Fig. 4 shows the Raman spectrum of carbon coated stainless steel 316L.



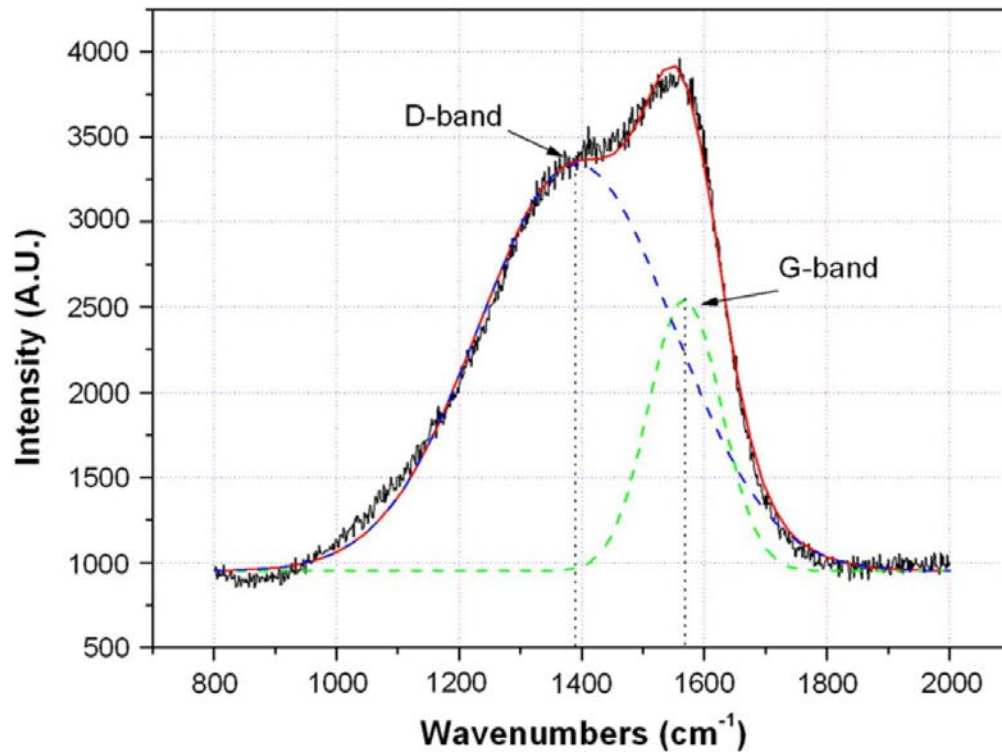


Fig. 4. Carbon on stainless steel 316L [authorization to reproduce obtained from ref. 34]

The G – band from Fig. 4 is at almost  $1568\text{cm}^{-1}$  as well as the D – band at  $1390\text{ cm}^{-1}$ . A suggestion has been made that the D peak intensity to the G - peak must have a relation that is linear to the graphite crystallite size. The magnitude of the D – band is bigger compared to the G – band. This means the crystallites for the graphite is small but disordered band is large. Another suggestion has also been made that the G and D peak are as a result of  $\text{sp}^2$  only. Feng et al [31] further determined the potentiodynamic polarization characteristics for uncoated as well as the carbon coated stainless steel 316L in 0.5 M sulfuric acid using 2ppm HF at  $80^\circ\text{C}$  and the results obtained is captured in Fig. 5.

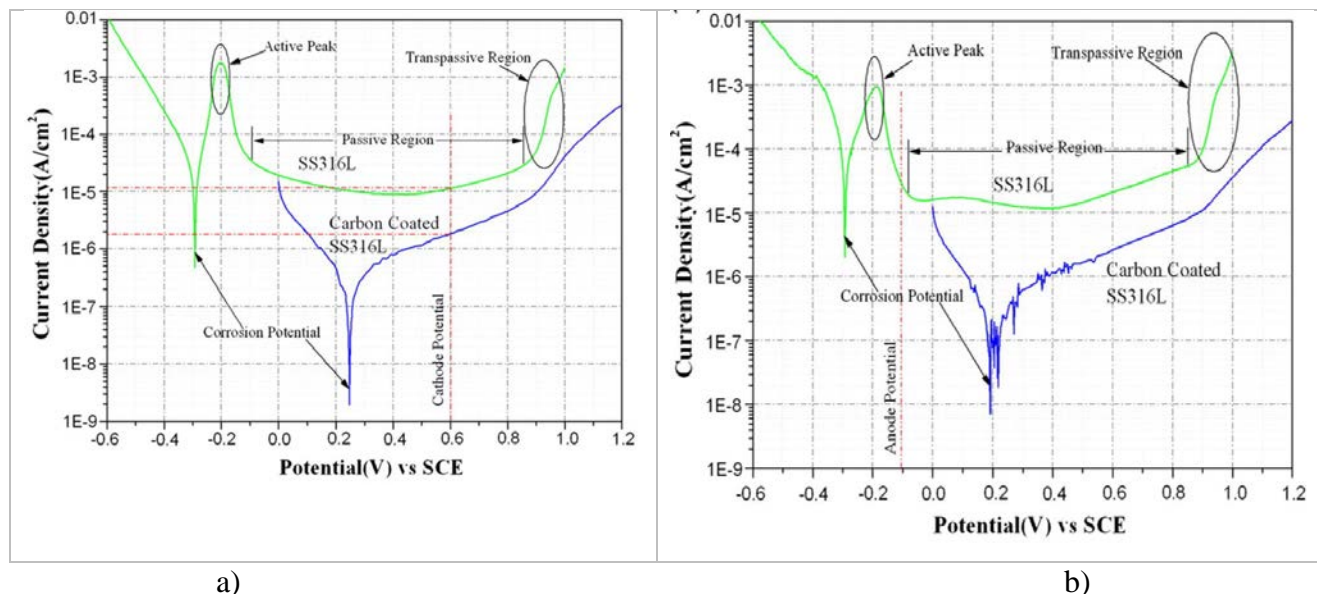
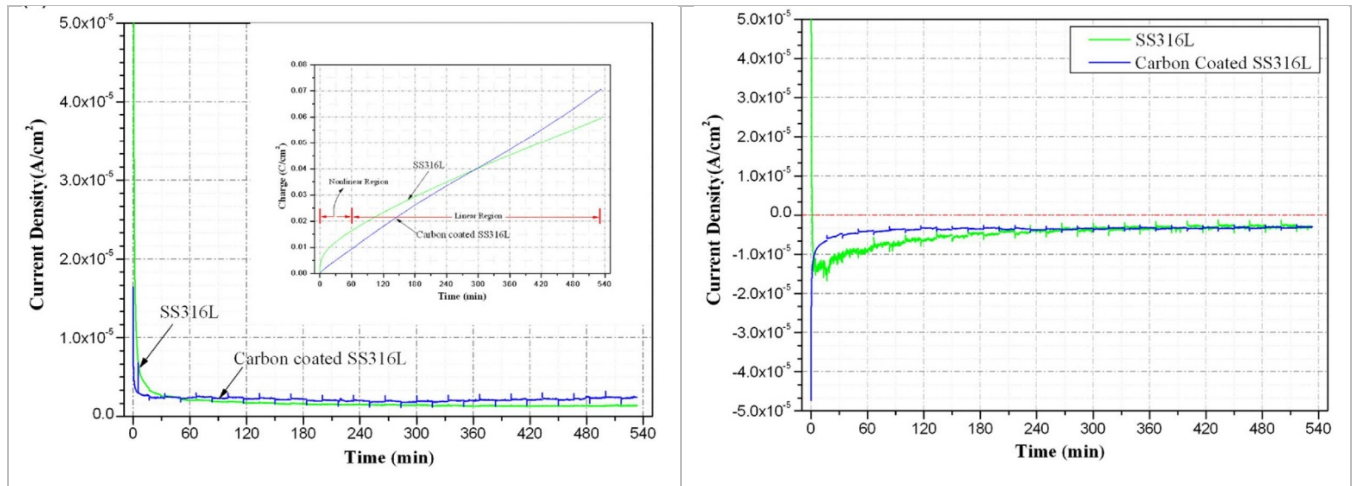


Fig. 5: The uncoated and carbon coated SS316L potentiodynamic curves in 0.5M in Sulfuric acid solution using 2ppm HF at a temperature of 80°C purged with a) air b) hydrogen [authorization to reproduce obtained from ref. 31]

The potentials for the corrosion of the stainless steel 316L at cathodic as well as anodic region of the fuel cell according to their findings was -0.286V against saturated calomel electrode as well as - 0.307 against saturated calomel electrode respectively. Half – cell potential for e (O<sub>2</sub>/H<sub>2</sub>O) [O<sub>2</sub> + 4H<sup>+</sup> + 4e<sup>-</sup> 2H<sub>2</sub>O] is always higher than that of e (H<sup>+</sup>/H<sub>2</sub>) [2H<sup>+</sup> + 2e<sup>-</sup> H<sub>2</sub>], the rate of corrosion potential of SS316L is always higher at the cathodic region and in the anodic region of the fuel cell. A passive thin film is also created on the surface. Corrosion potential for the stainless steel 316L which was carbon coated was observed to be nobler compared to that of bare stainless steel 316L (247mV against saturated calomel electrode and 192mV against saturated calomel electrode in the cathodic and anodic conditions respectively. When the corrosion potential is high, the chemical inertness also goes high and this implies good corrosion resistance. The polarization curve obtained for the bare SS316L was similar to austenitic SS. This can further be divided into 3 main regions that is, active area, passive area and trans passive area. Their investigation showed a high passivating current of 1mAcm<sup>-2</sup> as captured in Fig. 5 because of active dissolution and oxidation of the metal. In a situation where the potential is increased to 0.9 V against SCE, there was a boost in the current density due to the oxidation of Cr<sup>3+</sup> (Cr<sup>3+</sup> Cr<sup>6+</sup>). Main difference in carbon coated Stainless steel 316L is that there is no passive

region for carbon coated SS316L. The potentiodynamic curves using air to excite the PEM fuel cell cathodic region is also captured in Fig.10. Red dotted line shows the cathode operational potential at 0.6V against saturated calomel electrode while the current density for passivation of the stainless steel 316L at the cathodic region is  $11.26\mu\text{Acm}^{-2}$  but the current density of stainless steel 316L coated using carbon decreases to  $1.85\mu\text{Acm}^{-2}$ . When the current density for the anode is small, the rate of corrosion is low signifying the durability of the material. The potentiodynamic polarization curve based on their investigation is showed in Fig. 5 b. Flow plate for PEMFC corrodes when a potential is applied to it (cathode 0.6V against SCE and -0.1 V against Saturated calomel electrode). Feng et al [31] further did a potentiostatic test to ascertain the resistance to corrosion for PEMFC conditions. At the cathodic region, a 0.6V against saturated calomel electrode was used during the potentiostatic experiment and purged using air while at the anodic region, a -0.1V against saturated calomel electrode was applied while purging with hydrogen. The potentiostatic curve they obtained at 0.6V against SCE for bare as well as coated SS316L sample is also presented in Fig. 5. The current density of bare/uncoated stainless steel 316L reduces appreciably at the initial stages but stabilizes at  $1.4\mu\text{Acm}^{-2}$  from Fig. 5. The reduction in the current density was due to the formation of a passive film on the material being investigated. Comparing current densities for the potentiostatic and potentiodynamic test exhibited some differences attributed to the passive film. Accumulated charge for the uncoated SS316L as well as carbon coated SS316L is also shown in Fig. 6 insert. It can also be observed that there is correlation between charge as well as time and this is linear. The current stabilization (total passivation) can therefore be deduced to occur after nearly an hour. The current density stabilizes faster for the carbon coated stainless steel 316L and kept constant at  $2.4\mu\text{Acm}^{-2}$  [32]. There is a linear correlation observed during the testing time from the charge time curve showing that passivation is halted when the coated stainless steel 316L was investigated. This caused stability in the PEM fuel cell cathodic region. Current density of SS316L according to the investigation is less compared to the carbon coated in the stainless steel 316L in the potentiostatic experiment. The passive film created on stainless steel decreases corrosion rate.



a)

b)

Fig. 6: Bare and coated stainless steel 316L potentiodynamic graph a) Simulated cathodic region b) anodic condition (authorization to reproduce obtained from ref. [31]).

Figure. 6(b) explains the potentiostatic experiment for -0.1V against saturated calomel electrode generated from uncoated and coated stainless steel 316L using carbon around the anodic region. Decay of the current density for the SS316L was very rapid, underwent a positive negative switch as well as slowly. It shows initial passive film on the uncoated Stainless steel 316L was unstable within the PEM fuel cell. Fig. 7 shows the surface topology micrographs for the coated and uncoated carbon.

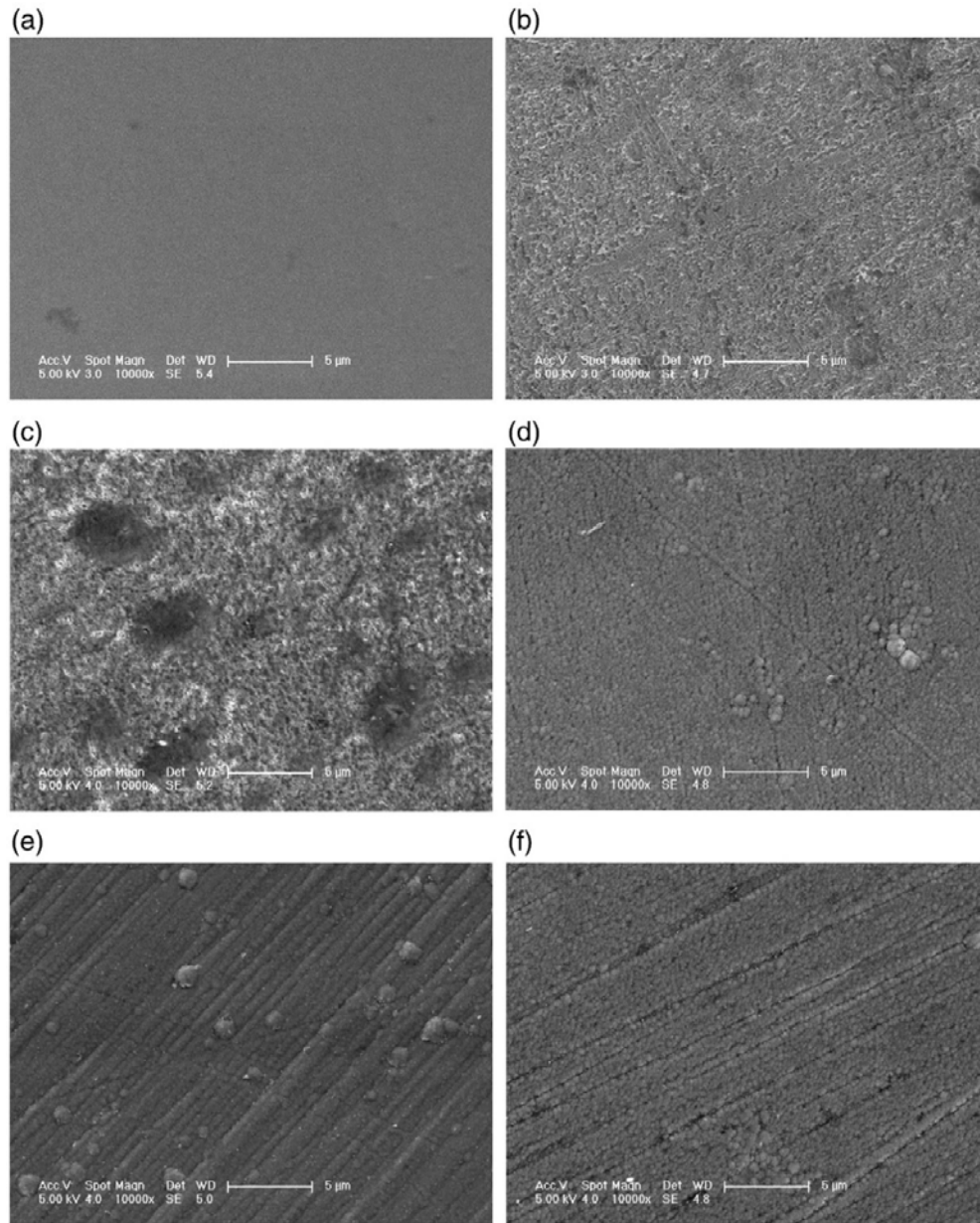


Fig. 7: Surface topology micrographs for the uncoated and coated Stainless steel 316L (authorization to reproduce obtained from ref. [33])

Feng et al [31, 34] further observed the uncoated and coated stainless steel 316L after the potentiodynamic investigation by adopting the SEM techniques. Rate of corrosion for the bare SS316L was high at both electrodes of the fuel cell (Anode and Cathode). Fig. 7 (b) shows the various corroded cells on stainless steel 316L after the polarization at the cathodic region of the fuel cell but the corrosion layer formed on the surface. Topology of the surface for coated SS316L did not exhibit any disparity but whitish substances were noticed on the samples shown

in Fig. 7(d) to (f). It implies that steel made of carbon is stable and is capable of serving as a layer to withstand corrosion. Fig. 8: shows the ICR results obtained.

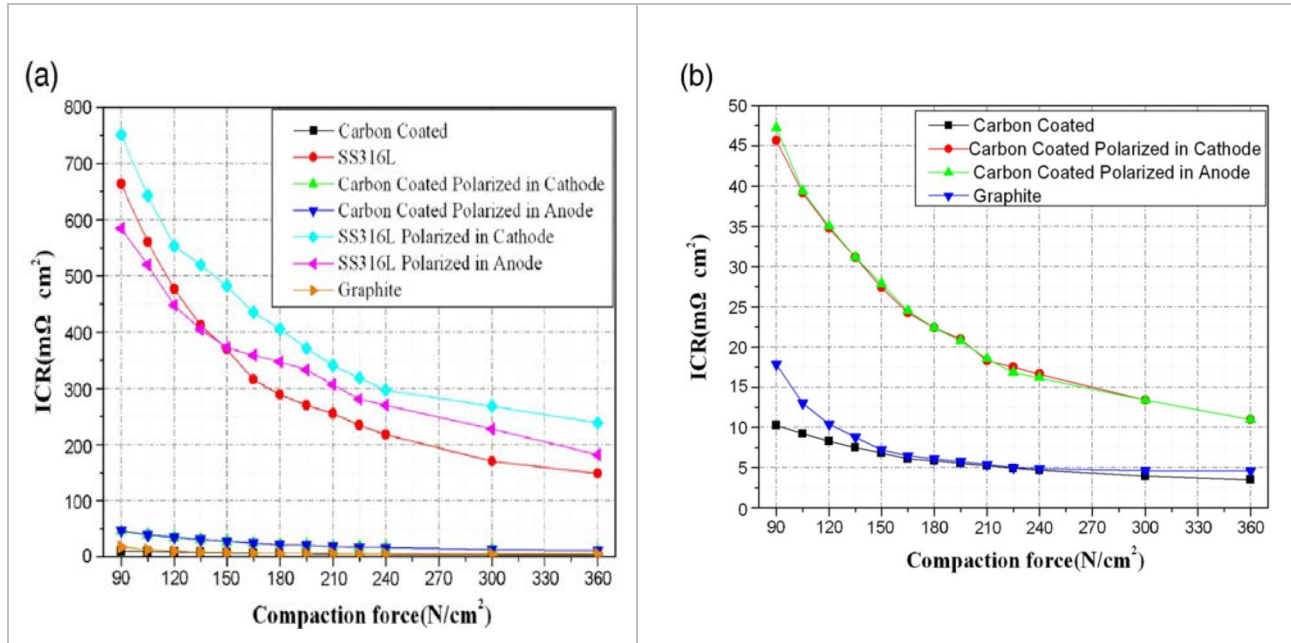


Fig. 8: Interfacial contact resistance against compaction force for a) coated and uncoated SS316L b) carbon coated stainless steel 316L after the potentiostatic test (authorization to reproduce obtained from ref. [31]).

Li et al [35] also conducted several experiments on aluminum bipolar plate to increase their ability to resist corrosion as well as improve the conductivity of the flow plate electrically. It must be noted that aluminum flow plates are 65% lighter compared to stainless steel. They deposited different kinds of coatings on the aluminum bipolar plate (Titanium Nitride, Chromium Nitride, Carbon, Carbon/Titanium Nitride and Chromium/Chromium Nitride). Aluminum alloy 5052 (AA – 5052) was used. Results obtained from the SEM showed that the coat made of carbon layer is denser compared to Titanium Nitride and Chromium Nitride. Potentiodynamic test showed that there was some improvement with the corrosion resistance for all the coatings. A detailed comparison for all the SEM images they obtained after the potentiostatic test, C/CrN and concluded that the multilayer coating shows the best stability. The chemical composition of the AA – 5052 they used is as shown in Table 2. Samples were split into 12mm x 12mm with thickness of 4mm and polished up using water proof abrasive paper.

Table 2. Aluminum alloy 5052 chemical composition

Magnesium	Silicon	Copper	Zinc	Manganese	Chromium	Iron	Aluminum
2.2-2.8	0.25	0.10	0.10	0.10	0.15-0.35	0.40	obtained

Fig. 9 shows the morphology of Titanium Nitride, Chromium Nitride, Carbon, Carbon/Titanium Nitride and Carbon/Chromium Nitride from a field emission scanning electron microscopy. To determine corrosion on the sample, the surface morphology technique was done after the potentiostatic tests. Fig. 10 shows the scanning electron microscopy (a) Titanium Nitride, (b) Chromium Nitride, (c) Carbon film, (d) Chromium/Titanium Nitride film, (e) Chromium/Chromium Nitride film. The characteristics of the uncoated and coated Aluminum alloy-5052 were determined using an acidic medium [35]. The electrochemical verification was done around 70°C to stimulate the PEM fuel cell. Stimulation of the cathode region was done by purging the solution using air before and during the test [32]. Again, to ascertain the electrochemical stability, the potential against time was registered for an hour [34].



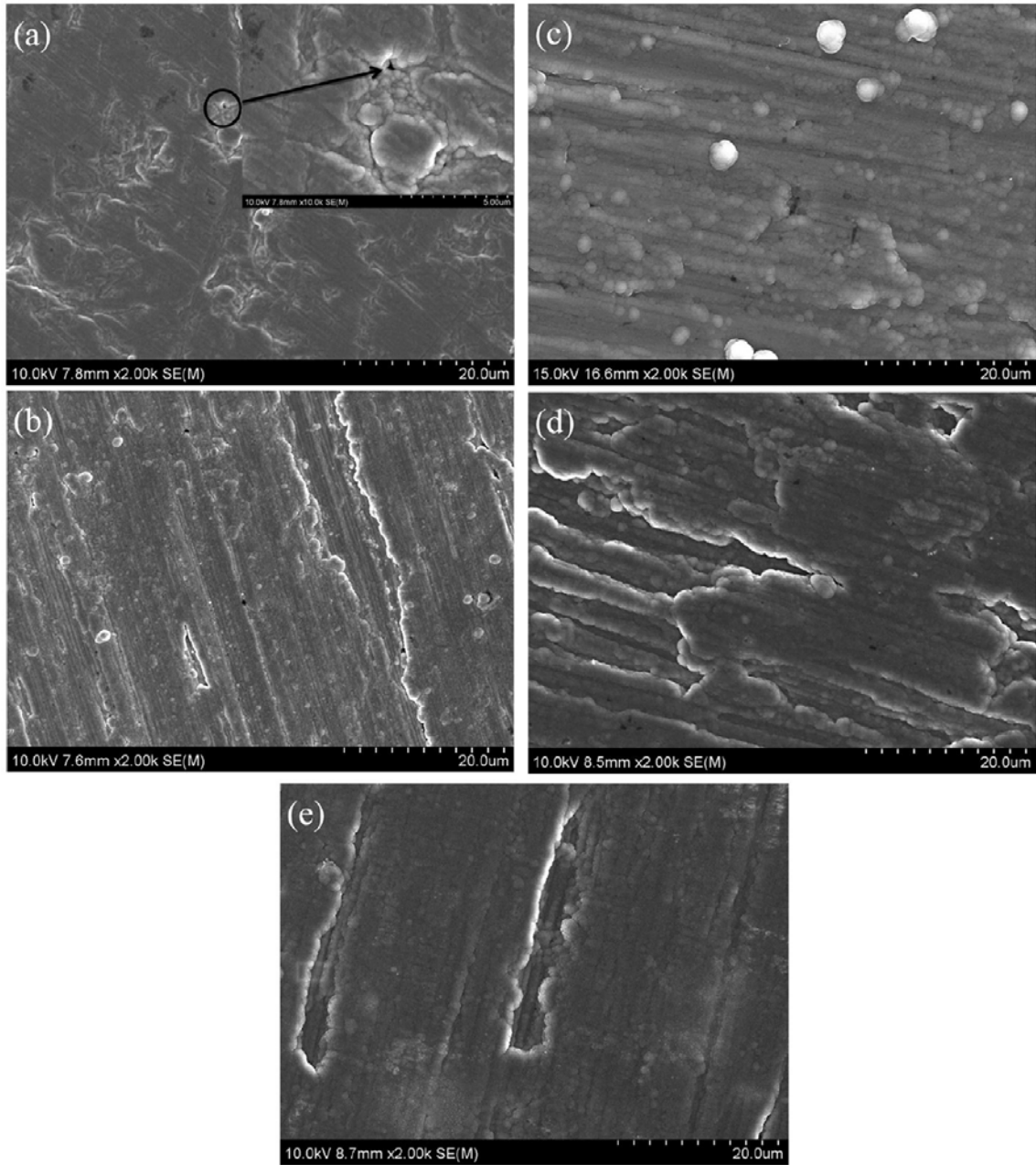


Fig. 9: Scanning Electron Microscopy image for (a) Titanium Nitride, (b) Chromium Nitride, (c) Carbon film, (d) Carbon/Titanium Nitride film, (e) Chromium/Chromium Nitride film (authorization to reproduce obtained from ref. [32]).



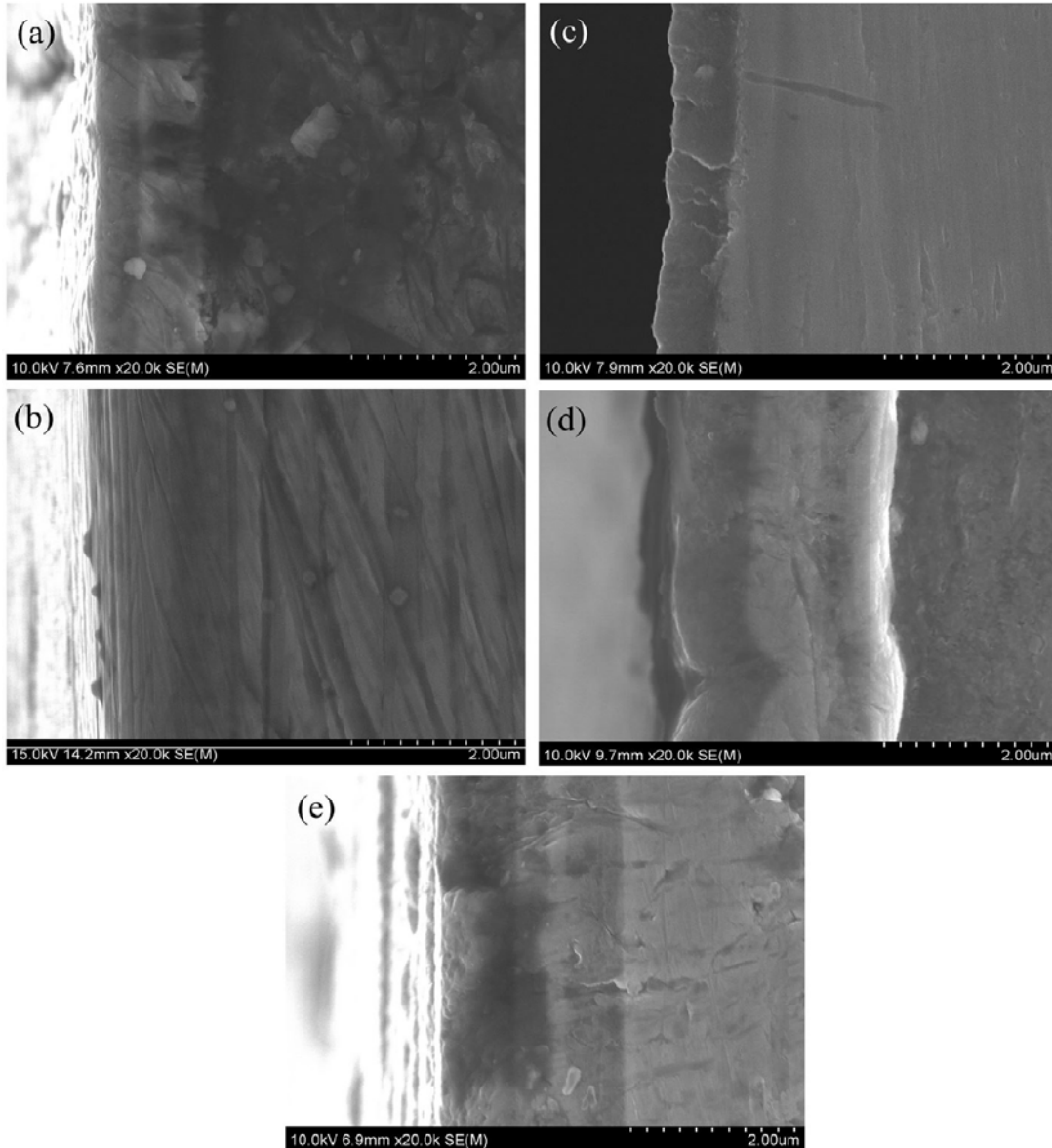


Fig. 10: Sectional Scanning Electron images for (a) Titanium Nitride, (b) Chromium Nitride, (c) Carbon film, (d) Carbon/Titanium Nitride film, (e) Chromium/Chromium Nitride film (authorization to reproduce obtained from ref. [32]).

Li et al [35] also measured the interfacial contact resistance for coated Aluminum alloy – 5052. The structure was made of Toray TGP – H – 090) which is a conducting carbon paper placed between the sample and 2 Cu plates. The drop in voltage is summing all the ICRs each sample found in the set up. In coating, the usual expectations are to have a dense, smooth as well as homogenous coating layer on the sample especially for physical vapour deposition coatings. This helps the ability for the material to resist corrosion to increase. Fig. 9 shows the image of

Titanium Nitride, Chromium Nitride, Carbon, Carbon/Titanium Nitride and Carbon/Chromium Nitride obtained from SEM. It is observed that there are some defects and pinholes on the Titanium Nitride and Chromium Nitride layers captured in Fig. 9 (a) and Fig. 10(b). Observable defects reduced the corrosion resistance of the Aluminum Alloy – 5052. Titanium Nitride as well as Chromium Nitride coatings were less dense than that of carbon coatings with spherical carbon granules. Li et al [35] further argued that even though the surface of the multi-layer is usually rough because of the Titanium Nitride and Chromium Nitride coatings being uneven, multilayer can create pinholes. The Carbon/Chromium Nickel multilayer coating was seen to be homogenous compared to Carbon/Titanium Nickel multilayer shown in Fig. 9 (d) and (e). The sectional images for the various coatings are shown in Fig. 10. The thickness for Titanium Nitride, Chromium Nitride, Carbon, Carbon/Titanium Nitride and Carbon/Chromium Nitride were 1.5mm, 1.3mm, 0.8mm, 2.5mm and 2.2mm respectively. The potentiodynamic curves for the bare and coated Aluminum Alloy – 5052 material for PEM fuel cell conditions is captured in Fig. 11. Most negative corrosion potential was observed for the uncoated AA-5052 which was nearly 1.4V against MSE. Corrosion potential for the coated AA-5052 was noble compared to the uncoated one implying that the AA – 5052 can resist corrosion better than uncoated AA – 5052 and the same was also observed for the chemical inertness.

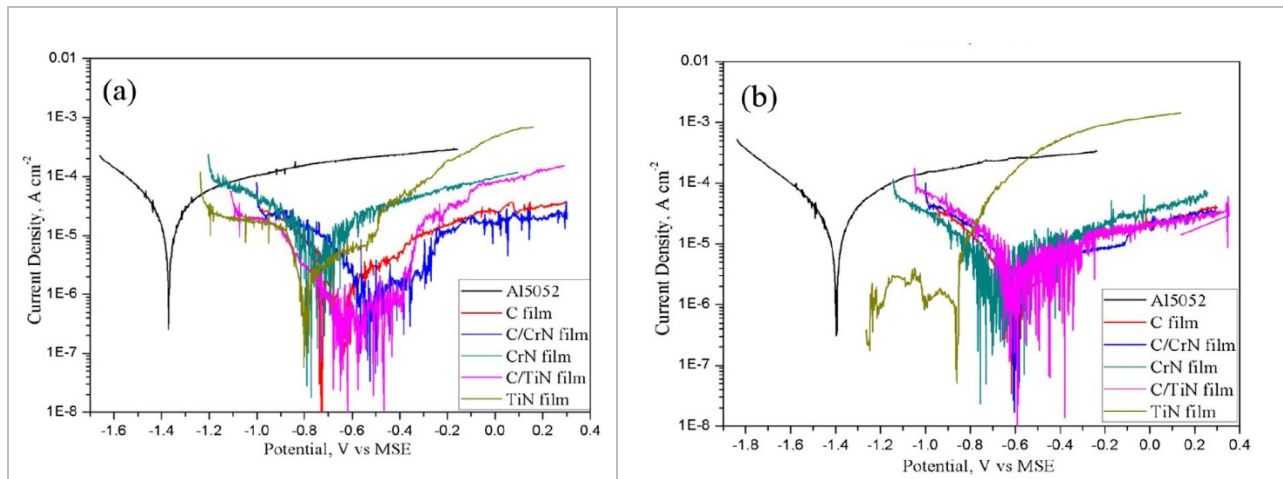


Fig. 11: The potentiodynamic curves for the coated and uncoated AA-5052 in proton exchange membrane fuel cell a) purged with H<sub>2</sub> (anodic conditions) b) purged with air (cathode conditions) (authorization to reproduce obtained from ref. [31])

## 1.2 Chromium coatings:

As explained earlier chromium nitride (CrN) is one of the types of coatings applicable to stainless steel as well because it reduces the  $I_{\text{Corr}}$  and ICR [31, 34]. Park et al [30] carried out experiment to examine the strength for Stainless steel 430 metal BP after applying a coat using Chromium Nitride/Chromium for Direct Methanol Fuel cells. It was observed according to the investigation that the Chromium Nitride/Chromium coated sample reduced the Interfacial Contact Resistance from  $200\text{m}\Omega\text{cm}^{-2}$  for uncoated Stainless Steel 430 to  $4\text{m}\Omega\text{cm}^{-2}$  for the Chromium Nitride/Chromium coated SS430).  $I_{\text{Corr}}$  was nearly  $10^{-5}\text{mAcm}^{-2}$  in uncoated stainless steel 430 as well as  $10^{-7} - 10^{-6}\text{mAcm}^{-2}$  for the coated Stainless Steel 430. Using the process of nitridation of alloys made of Chromium such as Nickel Chromium alloys and ferritic Chromium stainless steel, Brady et al [42] tried by means of experiment to reduce the ICR. Well-known method of creating coats on stainless steel is by Chemical vapour deposition and Physical Vapour deposition [36]. The process of modifying the surface using heat nitridation is an approach of reducing the  $I_{\text{Corr}}$  and ICR of BP forming a mixture of nitride/Chromium-nitride/oxide. When temperatures are high ( $900^{\circ}\text{C}$ ), thermal nitridation generates Chromium Nitrides that are discrete. This results in chromium depleted areas, reducing the opposition to corrosion. Precipitations such as Chromium Nitrides and Titanium Nitride as well as Chromium – depleted regions are more conductive compared to Chromium oxide. This is created when the nitridation occurs at high temperature. This explains that at very high temperature nitridation reduces the ICR. There is absence of Chromium from the matrix at high temperature conditions and this reduces the corrosion resistance. Atomic diffusion reduces whenever the nitridation temperature reduces which in effect reduces the thickness of the coat. This in effect causes the corrosion current density to increase as well as the ICR [37]. They therefore explained that the nitridation temperature must be optimized. The investigations conducted by M.J. Kelly, et al [38] considered the thermal nitridation for two separate temperatures ( $700^{\circ}\text{C}$  and  $900^{\circ}\text{C}$ ) stainless steel. Their report suggested that the ICR for stainless steel reduced after nitridation. This reduces the contact electrical resistance. At  $700^{\circ}\text{C}$  the coated steel according to their investigation had the best corrosion properties in PEM fuel cell conditions but coated steel at  $900^{\circ}\text{C}$  had relatively low properties. The explanation they gave was that at low temperatures, stainless steel nitridation created a layer and this protected the metal beneath the coat from the possibility of corroding. An explained was also given that the interfacial contact resistance value

and  $I_{\text{Corr}}$  simulated anode conditions and  $I_{\text{Corr}}$  in simulated cathode conditions for SS446M that has undergone nitridation but at low temperature was  $6\text{m}\Omega\text{cm}^{-2}$ ,  $1 \times 10^{-6}\text{Acm}^{-2}$  and  $1 \times 10^{-7}\text{Acm}^{-2}$  respectively and these are less compared to the bare SS446M. Another researcher also reported that that the ICR can also be reduced further to  $10 \text{ m}\Omega\text{cm}^{-2}$  using plasma nitridation of SS316L at  $370^{\circ}\text{C}$  for over two hours and that of SS304L as well but the  $I_{\text{Corr}}$  was higher than  $10\text{mAcm}^{-2}$ . Tina et al also projected that performing coating at higher temperature of  $370^{\circ}\text{C}$  will lead to precipitation hence an increase in depletion and reduced resistance to corrosion. Optimization of the temperature of nitridation of stainless steel 316L was performed by Hong et al. They varied the temperatures at which the coating was done between 257, 317 and  $377^{\circ}\text{C}$ . Smallest value for the Interfacial contact resistance obtained at a temperature of  $317^{\circ}\text{C}$  was  $13 \text{ m}\Omega\text{cm}^{-2}$  while the smallest value for the current density was obtained at  $257^{\circ}\text{C}$  ( $3.43 \times 10^{-6} \text{ Acm}^{-2}$  at  $0.6\text{V}$ ). The outcome of their investigations confirms the fact that optimizing the temperature of coating process reduces the Interfacial Contact Resistance. The process temperature can also be reduced using high – density plasma nitriding and this in effect nullify the Cr depletion [37]. Other authors investigated the merits of treating stainless steel 316L at lower temperatures for 180 minutes at  $900^{\circ}\text{C}$  using chromium. Using shot peening to active surface method helped the substrate to be pretreated and reduced the chromizing temperature. The  $I_{\text{Corr}}$  for the chromized SS316L was  $3 \times 10^{-7}\text{Acm}^{-2}$  and the ICR values was  $23 \text{ m}\Omega\text{cm}^{-2}$  and these values were 3 times less than that of bare SS316L [38 – 45]. A homogenous and heavy coat made of chromium on 1045 steel also investigated by Bai et al. Outcome of their investigation revealed that the phases of the material were made of carbides as well as chromium ferritic oxides [46]. Power density produced using the metal BPs was greater than that of graphite flow plates. They argued that carbon steel can be compared to that of graphite for the manufacturing of bipolar plates in PEM fuel cell. The price tag of carbon steel bipolar plates is less compared to metal bipolar plates. Other researchers also conducted investigations using chromium carbide on aluminum as well as stainless steel 316 samples. Their report exposed the fact that using chromium carbide gave a relatively reduced ICR as well as good resistance to corrosion. Testing the longevity of fuel cell using aluminum that is coated as bipolar plate at cell temperature of  $70^{\circ}\text{C}$  gave a minimum power degradation because of the corrosion of the metal. The behavior of some coatings electrochemically like Chromium Nitride/Titanium Nitride on Stainless steel 316L was also investigated. The work was aimed at examining Chromium/Nitride/Titanium Nitride coat on

stainless steel 316L. Protective efficiency ( $0.76 \text{ mAcm}^{-2}$ ) according to the electrochemical investigations was high when the coating of Chromium Nitride/ Titanium Nitride thickness was kept at 1:9. Another investigator examined Nickel – Chromium on Stainless steel 316L and concluded that the interfacial contact resistance reduced from 380 to  $200 \text{ m}\Omega\text{cm}^{-2}$  for the Nickel Chromium – coated Stainless Steel 316L after polarization [45].

### 1.3 Coatings containing Nitrogen

Coatings containing Nitrogen like Titanium Nitrides on stainless steel is very common [51]. Using Titanium Nitride coated SS304 as bipolar plate has also been investigated. Titanium Nitrides and Titanium (II) Nitrides ( $\text{Ti}_2\text{N}$ ) coatings gave a lower interfacial contact resistance, 25 and  $26 \text{ m}\Omega\text{cm}^{-2}$  respectively. A reduced  $I_{\text{Corr}}$  of 0.0131 and  $0.0145 \text{ }\mu\text{Acm}^{-2}$ . To effectively validate the results, the test must be conducted for longer period of time. Several protective coatings were deposited on stainless steel samples (stainless steel 304, stainless steel 310 and stainless steel 316) using PVD approach [52]. The outcome of the investigation met the target set by the DOE for bipolar. Interfacial contact resistance for the stainless steel 316L ( $300 \text{ m}\Omega\text{cm}^{-2}$ ), Zirconium – coated stainless steel ( $1000 \text{ m}\Omega\text{cm}^{-2}$ ) and Zirconium Nitride -coated stainless steel ( $160 \text{ m}\Omega\text{cm}^{-2}$ ) showed that even though Zirconium is good as coating material to combat corrosion, the interfacial contact resistance increases. Again, coatings made of Au reduces  $I_{\text{Corr}}$  and ICR less than the criteria set by the DOE as long as the thickness of gold coating is greater than 10nm especially on the cathode region. Some results also showed that Chromium Nitride is the best types of coat for SS BP of PEM fuel cells [53-55].

### 1.4 Ni – P electroless plating

Electroless plating technique is one strategy for coating BP. The industry is one of the sectors where Ni – P coating on stainless steel can be found. Using expensive organic material is one of the reasons why this method according to the research community is not the very best approach of coating even though it is simple and requires uniform solution bath at specific temperature and power of hydrogen. Homogeneity of the thickness of the coat via electroless approach is more compared to electroplating. Electroless plating approach was used to coat Ni – P on stainless steel 316L. Potentiostatic test using Ni – P made under favorable conditions were performed [56]. A negative current was generated for all times showing the cathode being protected. There

were no metal ions identified in the solution even after hours of potentiostatic treatment. Bulk resistance is reduced whenever the bipolar plate made of stainless steel was coated using Ni-P layer and the performance of the cell increased compared to existing cells on the market. The Ni-P coat on stainless steel 316L by Copper - interlayer showed maximum output current when compared to the proton exchange membrane fuel cell. A researcher conducted an intensive investigation coating AA 5251 using Ni - P and Ni - Co - P by means of electroless and electroplating approach. The corrosion current of Ni-Co-P coated increase by nearly 4 times compared to the bare AA5251 material. Corrosion current using electroless and electroplating approach were  $3.21 \times 10^{-5} \text{Acm}^{-2}$  and Ni - P was  $1.13 \times 10^{-7} \text{Acm}^{-2}$ . The ICR values was very high when the electroless method was used ( $114 \text{ m}\Omega\text{cm}^{-2}$ ) and this is higher compared to the values obtained using electroplating ( $\text{m}\Omega\text{cm}^{-2}$ ). Their investigation showed that using Ni-P coating was not the best for bipolar plates [57- 60].

#### 1.5 Coating using Noble metals

Gold, silver and platinum are noble metals that are suitable as coating materials on stainless steel due to the protection being provided by them as well as improving the conductivity of the stainless steel. Silver has good electrical conductivity, excellent corrosion resistance and very cheap. Through the process of ion implantation, a group of researchers coated a thin layer of silver on SS316L. According to the results they obtained from the potentiostatic tests, there was a reduction in the  $I_{\text{Corr}}$  from 10 to  $0.7 \mu\text{Acm}^{-2}$  after the implantation using Ag. Their work also showed an improvement of the ICR values from 312 to  $78 \text{ m}\Omega\text{cm}^{-2}$ . It must be noted that the value for the ICR can reduce immensely due to the method of coating, environmental conditions during the coating, as well as thickness of the coating [61- 64].

#### 1.6 Different coating materials

ICR characteristics of Niobium - implanted SS316L was investigated [31]. Results obtained showed that the current density of Niobium implanted Stainless steel 316L reduced in simulation in PEM fuel cell environment far below  $1 \mu\text{Acm}^{-2}$ . The dissolution rate from the induced coupled plasma results showed that the Niobium - implantation reduced. Depth profiles for XPS techniques showed that a passive film is created made of NbO. The outcome of their investigation showed that using Niobium improved the corrosion resistance as well as the flow of

electricity of Stainless Steel 316L in PEM fuel environment under simulated conditions. Their report did not consider the ICR test [65]. Another method that can reduce the corrosion resistance and interfacial contact resistance is doping using another element. Cerium element was used by Lavigne et al on the surface of stainless steel 316L. The steel surface was initially modified by keeping it in a steel solution made of  $\text{CeO}_8\text{S}_2$  and  $\text{Na}_2\text{SO}_4$  for two hours. The final data they collected from their investigation also showed that the Ce-modified stainless steel was less than the DOE criteria. There was also reduction in the ICR values they obtained from  $152 \text{ m}\Omega\text{cm}^{-2}$  for SS316L to  $33 \text{ m}\Omega\text{cm}^{-2}$  for the modified stainless steel [66].

#### 1.7 Coatings made of Nonferrous alloy.

Except for the price, Ni-based alloys are good coating material for metal bipolar plates. Monel, Hastelloy and Incoloy are examples of these materials. Ferrous alloys have low corrosion resistance as well as low ICR [67]. Cost of Ni-based alloys are higher than that of ferrous alloys. The variation in prices for Ni – based and ferrous alloys makes manufacturers of BPs prefer the latter for commercial applications. The cost, weight, accessibility and stampability of aluminum alloy makes them preferable by the research community as the best coating material but they are weak in strength compared to SS. Titanium is expensive but possess low corrosion resistance as well as low stampability when compared to stainless steel.

#### 1.8 Alloys made using Aluminum

Nitride coatings like Chromium Nitride and Zirconium Nitride on Al-5083 bipolar plates using Physical Vapour Deposition approach was examined thoroughly. The results obtained from the potentiodynamic curve depicted that aluminum – Chromium Nitride sample gave good corrosion resistance compared to Zirconium Nitride/Chromium Nitride coat under simulated conditions.

Multi layered bipolar plate is more fragile compared to the monolayer. A method of reducing the rate of corrosion for metal BPs is using composite layer. An Aluminum - based bipolar plate coated using polypropylene composite was also investigated by M.J. Kelly, et al [38]. The inter layer was made of carbon black and carbon paper. This was to lower the ICR between the aluminum and composite layer. Their work exposed the fact that the interfacial contact resistance was less than  $21 \text{ m}\Omega\text{cm}^{-2}$  as well as the  $I_{\text{Corr}}$  was less than  $1\mu\text{Acm}^{-2}$  [68]. Polymer based composite on Al was also researched using wet spraying [69]. Their investigation could not meet

the US department of Energy criteria because applying the coat by means of spray produced defects on the sample [70].

### 1.9 Alloys made of Nickel

Three commercial alloys were studied by Brady et al. These were Hastelloy G –30, Hastelloy G – 35 and AL 29 – 4C. The interfacial contact resistance of Al 29 – 4C, Hastelloy G-30 and Hastelloy G-35 reduced after nitridation to  $10 \text{ m}\Omega\text{cm}^{-2}$  (at  $150 \text{ Ncm}^{-2}$ ). Their surfaces became resistant to corrosion due to nitridation at the anodic current density falling below  $1\mu\text{Acm}^{-2}$ . Forming semi – continuous Chromium Nitride surface layers on (Hastelloy) and AL 29 – 4C via nitridation was also performed. The application of these metal bipolar plates is small because of their high price [69]. The resistance to corrosion on uncoated metals was equally investigated [70]. Their work showed that the current density of stainless steel 316L, stainless steel 321, stainless steel 347, Inconel 625, Incoloy 825, Hastelloy C-276, Tantalum and Titanium were 26, 8, 15.8, 4, 6.4, 4.8,  $1.26 \times 10^{-2}$  and  $1260\mu\text{Acm}^{-2}$  respectively. stainless steel 316L, stainless steel 321, stainless steel 347, Inconel 625, Incoloy 825 and HastelloyC-276 at  $80^\circ\text{C}$  was 12.6, 20, 50, 0.1, 4 as well as  $0.8\mu\text{Acm}^{-2}$  respectively. At  $120^\circ\text{C}$  only Tantalum and at  $80^\circ\text{C}$  Inconel 625 and HastelloyC-276 meet the standard set by the DOE ( $1\mu\text{Acm}^{-2}$ ). Tantalum has very high corrosion resistance but it is not a cheap metal (very expensive). The most suitable material for bipolar plates are HastelloyC-276 and Inconel625. From commercial perspective, stainless steel especially SS316L are conducive for the manufacturing of BP because their prices are lower, and they are also abundant [71]. The formability of Stainless Steel 316L is higher compared to other metals such as Titanium and this characteristics of stainless steel 316 aid in stampability.

#### 1.9.1 Titanium alloys

Titanium a type of metal which is very light (density  $4.51 \text{ gcm}^{-3}$ ). It has hexagonal close packed configuration. Titanium is normally coated using an oxide layer that is nonconductive. It must be noted that when Titanium is compared to some metals with Face Centered Cube structure for example, Nickel and stainless steel 316L, the formability of Titanium is low hence weaker stampability. The oxide layer coated on Titanium surface causes the interfacial contact resistance to increase considerably. The corrosion and conductive layers of Ti has been coated in several investigations conducted by several researchers in order to improve their performance. Using



pulsed bias arc ion plating approach, Titanium – Gold film was coated on Titanium samples which led to interfacial contact resistance as low as  $4.3 \text{ m}\Omega\text{cm}^{-2}$ . The current density of Titanium / Titanium – Gold was nearly  $10\mu\text{Acm}^{-2}$  and this is greater than the US, Department of Energy standard. Nitrogen plasma ion implantation was conducted at low temperature of  $100^\circ\text{C}$  and high temperature of  $370^\circ\text{C}$  in order to enhance the corrosion resistivity as well as ICR of titanium samples by Feng et al. [34].

## 2.0 Hydroforming – stamping of bipolar plates.

As explained earlier, graphite and polymer based composite material used for bipolar plates are fading away [35] and being replaced by metallic bipolar plates because the metallic sheets can be stamped up to low thickness below  $0.051\text{mm}$ . Laser welding process can be used in metallic bipolar plates making put them at a better advantage compared to the other materials. Two methods for creating channels on large materials to build flow plates for PEMFC applications is hydroforming and stamping. Fig. 12 shows the process of performing stamping while Fig. 13 shows hydroforming approach but there are two main observable defects using these two processes. These are, the breaking of the sample during the forming stage and unsteady distribution of flow. Channel rib depth is optimized to reduce the unsteady distribution of the flow [32]. A researcher concluded that the distribution of the flow is dependent on channel rib depth. Optimization of the depth therefore affects the distribution of the flow [66].

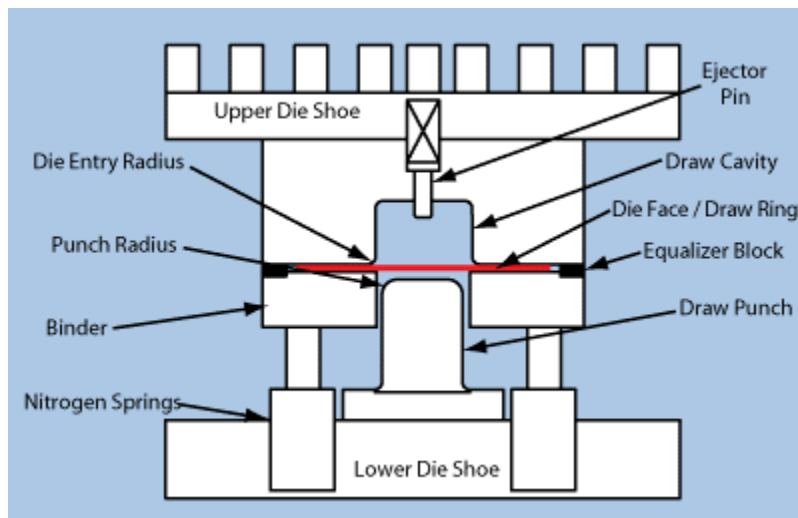


Fig. 12: Schematic diagram for the process of stamping (authorization to reproduce obtained from ref. [32])

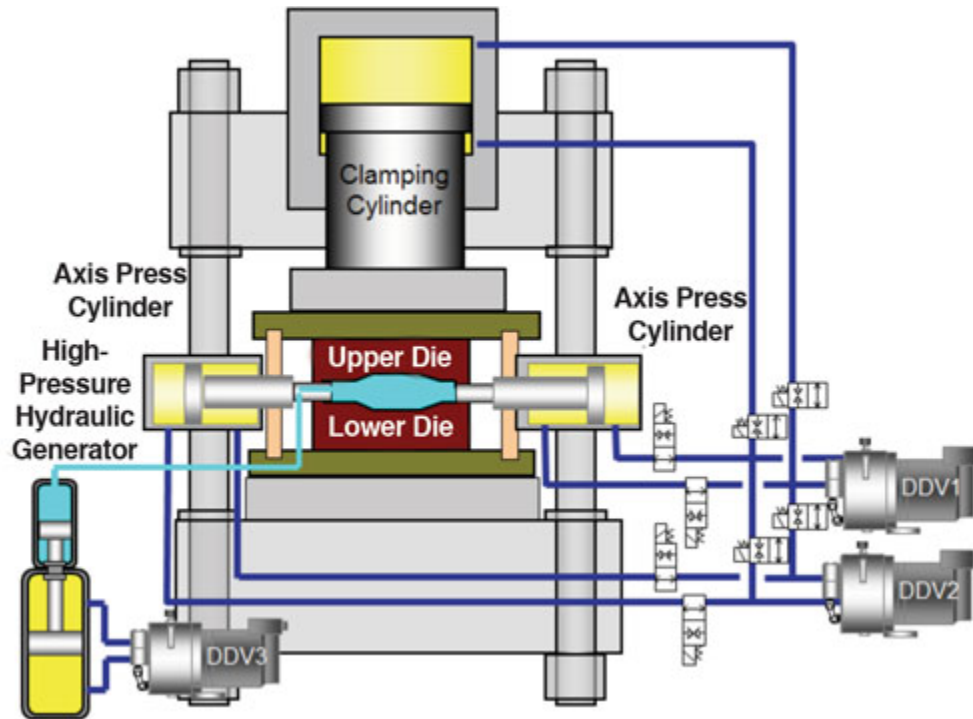


Fig. 16: Schematic diagram of a machine for the hydroforming process (authorization to reproduce obtained from ref. [33])

At the channels peak, the hydroformed bipolar plate yielded a low surface roughness value compared to the stamped bipolar plate. Again, hydroforming shown in Fig. 13 reduces dimensional variations compared to stamping process. There are two major concerns that must be addressed during the micro forming process and high production rate of bipolar plates. The dimensional error because of manufacturing technology controlled is the first issue. The next issue is related to shape error because of spring back in the stamping technique, stress in welding process, unequal and clamping pressure. To improve the efficiency of the cell, it is always recommended, that pressure dissemination via the cell is uniform. The dimensional error as well as the shape error all lead to the unsteady stress distribution hence the unbalanced distribution of flow also affects performance between the flow plate and Gas Diffusion Layers [33]. The variation of channels and ribs as well as the surface roughness are all classified under

dimensional error. The formability and contour of the surface as well as the quality of metal bipolar plate using stamping and hydroforming have all be researched. According to their investigations, hydroforming makes the bipolar plate have lower dimensional variations.

### 2.1 Bare Metals

A material classified under bare material is Stainless steels. This is because they possess good strength, stable chemically, flow of gas through them is low, many types of alloy choice as well as can be applied for mass production of the fuel cells and also relatively cheap. The major challenge using this material is corrosion. Different authors have considered using stainless steel as bipolar plate [31 – 33] and their investigation showed that the rate of corrosion is low and the output of the cell is very reliable for hours. Wang et al [73] conducted a research and also concluded that stainless steel is good for making of bipolar plates [74 – 75]. Their work showed that austenitic (349TM) and Ferritic (AISI446) stainless steel with high chromium content are good for bipolar plate material even though ferritic needs improvement.

### 2.2 Coated Metals

Nickle, titanium, stainless steel and aluminum are considered as suitable for BPs but to prevent corrosion, they must be coated using good coating covering. Coats applied on materials are supposed to be very conductive as well as stick to the metal substrate without showing the base metal out and they must also be very close to avert formation of micro – pores on the coated metal to reduce coating expanding [36]. Today two types of coatings are being investigated. These are coatings made of metals and carbons. Coatings made of carbon include usage of graphite, polymer, as well as mono polymers. The coatings made of metals involves the usage of metals that are noble. Today there are more research being conducted on coated stainless steel (316L) as bipolar plates [37,38]. An investigation conducted by wind et al shows that using BP that is gold coated stainless steel also improved the efficiency of the fuel cell just like graphite. Coating of stainless steel 316L was proposed by M.J. Kelly, et al [38]. Coating of metallic bipolar plates still have some challenges due to pinhole defects [40,41]. Brady et al [41, 42] as a way of curbing the impact of pinhole defect due to coating manufactured bipolar plate using thermal nitridation process. This approach is yet to be verified. Researchers around the world are

working to enhance the performance of the fuel cell via coating the BPs mostly for the automotive industry but they are yet to be commercialized.

### 3.0 Summary of surface treatment adopted for development of BPs.

Metallic BPs as explained are susceptible to corrosion and rust when their surface comes into contact with an environment that is acidic and moist especially as can be seen in fuel cells. The various research work that concerned coating of the metals by some individuals and research groups have been presented earlier but this part of the paper will give a summary of the current methods used in coating of bipolar plates. The methods considered are chemical, treatment using heat, spraying, vapor deposition, and Ion implantation approach.

#### 3.1 Chemical approach

The compositions from substrate to the final coated material metallurgically was studied electrochemically using passive film by a group of researchers and their work saw a high improvement of the bipolar plates corrosion resistance. Their approach made the surface morphology to become very smooth as well as glossy appearance and this enhanced the gas and H<sub>2</sub>O movement in the flow channels on the flow plate and decreases the resistance as a result of surface morphology. Electrochemical characteristics of the cell stack was also evaluated by another group of researchers and their work was directly linked to the working temperature and lesser impact on pressure [34]. There is the need for human intervention whenever coating process like cyclic voltammetry and electroplating process is being used. A solvent for the anode and cathode is also required. Using electrochemical approach as the method of coating gives varying  $I_{\text{corr}}$  or doping percentage. According to the DOE, chemical experiments must be conducted beyond 24hrs in solvent. The materials must be checked for the possibility of corrosion in a fuel cell. Electrochemically coating the material reduces the possibility of it becoming corroded over a period in harsh conditions. This process in effect will help reduce the manufacturing cost but the results obtained via this process are generally inconsistent.

#### 3.2 Treatment using heat

Traditional nitriding processes are plasma, gaseous and salt bath nitriding [76]. It is a commonly used thermochemical treatment method of applying a coat on metallic flow plates using nitrogen

and carbon (nitrocarburizing) [77, 78]. Diffusion on substrate of the metallic surfaces at temperatures between 480 and 580°C also occurs on the surface. The development of materials as well as expectations of the various components of the materials gave rise to several technological approaches being implemented. Some challenges of using plasma nitriding (NP) are arcing, hollow cathode effect, sputtering and corner. The corner effect is a phenomenal treatment process which involves plasma nitriding (PN), gas nitriding (GN) as well as carburizing. Another approach used in active screen plasma nitriding (ASPN) gave good results but to uniformly complete nitriding, enough bias activation is required. This implies that nitriding increases the corrosion resistance, surface hardness and fatigue strength. The merits of traditional PN without their demerits related to metals are all used in ASPN [79].

### 3.3 Ion implantation

This is a finishing approach utilized on the surfaces of metals using ionized atoms and some specific elements such as Nickel, Molybdenum, Chromium etc., extracted via electrical means, accelerated and geared towards the area being treated using vacuum chamber. The ions then perforate and become attached but there is loss of energy due to elastic collision with target atoms according to a research performed by Dearnaley, 2013 [76]. The performance of the implanted layer is higher because treatment depth very thin This method is described as the line of sight approach. There are other methods like metal dielectric deposition, plasma deposition, annealing and photolithography. The method results in smaller doses ( $10^{11}/\text{cm}^2$ ) compared to chemical deposition. Doses for various levels are regulated precisely using this approach and the doping uniformity is very constant. There is low possibility of contamination because the process is often carried out in a vacuum, but the approach involves the usage of expensive equipment amounting to millions of pounds. The passive layer composition modification using ion implantation method for 316L stainless steel flow plates has been researched thoroughly. Interfacial contact resistance also reduced appreciably from  $312\text{m}\Omega\text{cm}^{-2}$  to  $36\text{m}\Omega\text{cm}^{-2}$ . Co – implantation using Ni – Cr reduced the ICR from  $255\text{m}\Omega\text{cm}^{-2}$  to  $22\text{m}\Omega\text{cm}^{-2}$  as the resistance of the corrosion increased appreciably. The work done by another researchers, Zhang et al [90] also saw the  $I_{\text{Corr}}$  of the sample with a coating layer being kept at  $10^{-6.5}\text{Acm}^{-2}$  and the ICR for the sample being coated for the cathode conditions in a simulation process surged up appreciably from  $35\text{m}\Omega\text{cm}^{-2}$  to  $60\text{m}\Omega\text{cm}^{-2}$ . The work they conducted buttressed the fact that ion

implantation led to long term stability in proton exchange membrane conditions. The values obtained for ICR and  $I_{\text{corr}}$  are still greater than that of the target set by the US, DOE, which is  $10 \text{ m}\Omega\text{cm}^{-2}$  and  $1\mu\text{Acm}^{-2}$  though this approach improved the performance of the fuel cell successfully. There was good uniformity obtained from one wafer to the other giving a good flow channel purposely for equal distribution of reactant gases in PEM fuel cell.

### 3.4 Applying coat using spray

Spray gun is used during thermal spraying and air brushing to apply a coat on the surface of a metal. The material used for the coating sometimes comes as powder, ceramic rod as well as wire. Some investigators like Husby [77] employed the air brushing methods and the results generated for the current density values were between  $0.11\mu\text{Acm}^{-2}$  to  $0.54\text{cm}^{-2}$  for stainless steel flow plates. Results obtained had the best current density after the surface was coated and this met the target set by the DOE which is less than  $1\mu\text{Acm}^{-2}$ . Fabricated multilayer coated onto substrate can be done using this conventional air brush approach. The thickness of the coating, spraying time, gaps in between sample and the air brush as well as the temperature for the substrate have all been examined via air brushing approach. According to a research conducted by Susanna et al [78], the coated sample by means of spray had 270nm of thickness and 80nm as the roughness of the surface. The target distance was kept between 100 and 180nm, while the pressure was also maintained between 10 – 18 pound per square inch at ambient temperature to nearly  $70^\circ\text{C}$  and the spraying was performed for a period of 30 seconds. The combustion flames/electric arc are the main disparity between thermal spraying and other spraying processes. The  $I_{\text{corr}}$  results obtained according to an investigation carried out by Gago et al [79] is  $1.10 \times 10 \text{ Acm}^{-2}$  and although this value was low, it still could not meet the set target. The maximum thickness of the thermal spray on the metallic plate was maintained between 0.6 – 0.8nm. with the surface roughness between 4 – 15mm. A researcher also argued in his report that using arc process in thermal spraying resulted in some deposits on the metal surface and this enhanced the coating percentage which in effect gave good protection for the material especially in an aquatic environment. This also indicates excellent uniformity absorbance within the plates, which will reduce the possibility of the part coated from damaging [78].

### 3.5 Vapor deposition (VD)

The methodology used for coatings are same when using vapour deposition approach, but the technology utilized as well as the processes involved physically differ slightly. Heating or sputtering is employed to deposit layers on the substrate of a metal in physical vapour depositions (PVD). In terms of corrosion resistance, PVD coatings are better compared to electroplating process due to the hardness of coating when PVD approach is used. The  $I_{\text{Corr}}$  obtained using PVD coating was  $0.00029\mu\text{Acm}^{-2}$  which indicates good corrosion resistance compared to electroplating method which was  $1.9\mu\text{Acm}^{-2}$ . PVD method is less harmful to the environment compared to electroplating approach. Durability that covers topcoats are not needed in PVDS because abrasion resistance, temperature and strength are all excellent [80]. The corrosion resistance for the single layered coating of TiN and Graphite -  $i\text{C}^{\text{TM}}$  improved when the multilayer coated TiN + C was used. An investigation conducted also showed that 10nm Au coatings would be the best coating material for further future investigation. Chemical process is employed in the chemical vapour deposition (CVD) approach where high quality as well as good characteristics of a solid material is used as the material used for the coating process. The ICR and  $I_{\text{corr}}$  obtained falls within the US Department of Energy targets of  $<10\text{m}\Omega\text{cm}^{-2}$  and  $<1\mu\text{Acm}^{-2}$  whenever CVD approach is used. The inductive coupled plasma (ICP) combined with physical vapor deposition method of gas mixture ( $\text{TiCl}_4$ ,  $\text{BCl}_3$ ,  $\text{H}_2$  and Ar) was also investigated.  $\text{TiB}_2$  films were also seen as being very hard. It is cost saving and increases production. Again, the plasma surface alloying (PSA) approach is used in VD group [80 - 85]. The PSA using nitrides as well as carbon was also performed by Dong et al. The approach utilized enhanced resistance to corrosion on austenitic stainless steel. The usage of the PSA was also employed by Wang et al where they used Niobium and Carbon diffusion samples to treat materials to generate reduced current density ( $0.051\text{-}0.058\mu\text{Acm}^{-2}$ ) and interfacial contact resistance of  $8.47\text{m}\Omega\text{cm}^{-2}$  [86 - 89]. A new type of approach called hybrid plasma surfacing co – alloying approach was also investigated. Interfacial contact resistance values of the samples coated were  $9\text{m}\Omega\text{cm}^{-2}$  and long duration experiments were carried out to determine impact of corrosion on the cell stack. Another research conducted is using arc ion plating (AIP) [90]. The two experiments conducted by Zhang et al [91] using titanium and SS by the AIP approach concluded that nanocomposite Ti – Ag – N improved the resistance to corrosion as well as conductivity of the material. In extremely high oxidized atmosphere, titanium plate showed good resistance to corrosion, low



interfacial contact resistance at  $2 \text{ m}\Omega\text{cm}^{-2}$  under  $140 \text{ Ncm}^{-2}$  and this increased the electrical conductivity. The next investigation conducted was to enhance the performance by using  $\text{CrN}_{0.86}$  film coated stainless steel 316L flow plates that limited the interfacial contact resistance to  $8.8 \text{ m}\Omega\text{cm}^{-2}$  under  $100 \text{ Ncm}^{-2}$  and the  $I_{\text{CORR}}$  reached  $0.1 \mu\text{Acm}^{-2}$  [92, 93]. From the results obtained for the two-research conducted, it can be deduced that the high film density obtained using the arc ion plating was the main contributing factor to the high performance of the coated bipolar plates. Cooling water system is needed to discharge heat for VD technique in some special cases at extremely high temperature [94- 101].

#### 4.0 Conclusion

The investigation presented coating techniques and materials for PEM BPs. Several materials currently used for the manufacturing of fuel cell bipolar plate were discussed. Materials like composites are being encouraged by researchers in the manufacturing of bipolar plate because they reduce the weight of the cell. Even though metals and graphite continue to dominate the fuel cell market in terms of manufacturing of bipolar plates, researchers recommended that metals are coated to increase the longevity of the fuel cell. This will further reduce the prices of fuel cell in general. There is still more research work being conducted on metal and nonmetallic material to ascertain their overall effect on fuel cell performance. Optimization of all the surface treatment techniques captured in this report is still being researched to determine the best conditions that would yield the maximum performance of the fuel cell. A conclusion can therefore be deduced that for fuel cell to become commercially viable and to enhance their competition with other energy generation mediums for the automobile industry and portable applications, they must meet the target set by the US, Department of Energy. For the BPs to meet these criteria, coating becomes very necessary especially when they are made of metals. This improves the interfacial contact resistance, current density and the corrosion resistance.



## 8.0 Reference

- [1]. Tabbi Wilberforce, A. Alaswad, A. Palumbo, A. G. Olabi, Advances in stationary and portable fuel cell applications, *International Journal of Hydrogen Energy* 41(37) March 2016.
- [2]. Yifei Wang, Dennis Y.C.Leung, JinXuan, Huizhi, Wang. A review on unitized regenerative fuel cell technologies, part-A: Unitized regenerative proton exchange membrane fuel cells. *Renewable and Sustainable Energy Reviews*. Volume 65, November 2016, Pages 961-977. <https://doi.org/10.1016/j.rser.2016.07.046>
- [3]. Nicu Bizon, Phatiphat Thounthong. Real-time strategies to optimize the fueling of the fuel cell hybrid power source: A review of issues, challenges and a new approach. *Renewable and Sustainable Energy Reviews* Volume 91, August 2018, Pages 1089-1102. <https://doi.org/10.1016/j.rser.2018.04.045>
- [4]. T. Wilberforce, A. Al Makky, A. Baroutaji, R. Sambhi, A.G. Olabi, Computational Fluid Dynamic Simulation and modelling (CFX) of Flow Plate in PEM fuel cell using Aluminum Open Pore Cellular Foam Material, *Power and Energy Conference (TPEC), IEEE, Texas*. 2017. DOI: 10.1109/TPEC.2017.7868285.
- [5]. T. Wilberforce, Z. El-Hassan, F.N. Khatib, A. Al Makyy, A. Baroutaji, J. G. Carton and A. G. Olabi, Modelling and Simulation of Proton Exchange Membrane Fuel cell with Serpentine bipolar plate using MATLAB, *International journal of hydrogen*, 2017. DOI: 10.1016/j.ijhydene.2017.06.091.
- [6]. E.H.Majlan, D.Rohendi, W.R.W.Daud, T.Husaini, M.A.Haque. Electrode for proton exchange membrane fuel cells: A review. *Renewable and Sustainable Energy Reviews* Volume 89, June 2018, Pages 117-134. <https://doi.org/10.1016/j.rser.2018.03.007>
- [7]. K.Priya, K.Sathishkumar, N.Rajasekar. A comprehensive review on parameter estimation techniques for Proton Exchange Membrane fuel cell modelling. *Renewable and Sustainable Energy Reviews* Volume 93, October 2018, Pages 121-144. <https://doi.org/10.1016/j.rser.2018.05.017>
- [8]. M.R.Islam, B.Shabani, G.Rosengarten, J.Andrews. The potential of using nanofluids in PEM fuel cell cooling systems: A review. *Renewable and Sustainable Energy Reviews*. Volume 48, August 2015, Pages 523-539. <https://doi.org/10.1016/j.rser.2015.04.018>.

- [9]. Fabian Fischer. Photoelectrode, photovoltaic and photosynthetic microbial fuel cells. *Renewable and Sustainable Energy Reviews*. Volume 90, July 2018, Pages 16-27. <https://doi.org/10.1016/j.rser.2018.03.053>
- [10]. Tabbi Wilberforce, Zaki, El-Hassan, F.N. Khatib, A. Al Makyy, A. Baroutaji, J. G. Carton and A. G. Olabi. Developments of electric cars and fuel cell hydrogen electric cars. DOI: 10.1016/j.ijhydene.2017.07.054
- [11]. T. Wilberforce, A. Al Makky, A. Baroutaji, R. Sambhi and A.G Olabi, Optimization of bipolar plate through computational fluid dynamics simulation and modelling using nickel open pore cellular foam material, International conference on renewable energies and power quality (ICREPQ'17), ISSN 2171-038X, No 15 April 2017.
- [12]. Dilek Nur Ozen, Bora Timurkutluk, Kemal Altinisik. Effects of operation temperature and reactant gas humidity levels on performance of PEM fuel cells. *Renewable and Sustainable Energy Reviews*. *Renewable and Sustainable Energy Reviews* 59 (2016) 1298–1306. <https://doi.org/10.1016/j.rser.2016.01.040>.
- [13]. Bora Timurkutluk, Cigdem Timurkutluk, Mahmut D. Mat, Yuksel Kaplan. A review on cell/stack designs for high performance solid oxide fuel cells. *Renewable and Sustainable Energy Reviews* Volume 56, April 2016, Pages 1101-1121. <https://doi.org/10.1016/j.rser.2015.12.034>
- [14]. T. Wilberforce, A. Alaswad, J. Mooney and A. G. Olabi, Hydrogen Production for Solar Energy Storage. A Proposed Design Investigation, Proceedings of the 8<sup>th</sup> International Conference on sustainable Energy and Environmental Protection. ISBN: 978-1-903978-52-8. 2015.
- [15]. Tabbi Wilberforce, F. N. Khatib, Ahmed Al Makky, A. Baroutaji, A.G. Olabi . Characterisation Of Proton Exchange Membrane Fuel Cell Through Design Of Experiment (DOE). Proceedings of SEEP2017, 27-30 June 2017, Bled, Slovenia.
- [16]. Weng Cheong Tan, Lip Huat Saw, Hui San Thiam, Jin Xuan, Zuansi Cai, Ming Chian Yew. Overview of porous media/metal foam application in fuel cells and solar power systems. *Renewable and Sustainable Energy Reviews*. Volume 96, November 2018, Pages 181-197. <https://doi.org/10.1016/j.rser.2018.07.032>
- [17]. Tabbi Wilberforce, F. N. Khatib, O. Emmanuel, O. Ijeaodola, A. Abdulrahman, Ahmed Al Makky A. Baroutaji, A.G. Olabi. Experimental study of operational parameters on the performance of PEMFCs in dead end mode. Proceedings of SEEP 2017, 27-30 June 2017, Bled Slovenia.

- [18]. Daniel R. Dreyer, Sungjin Park, Christopher W. Bielawski and Rodney S. Ruoff. The Chemistry of Graphene Oxide, DOI: 10.1039/B917103G (CRITICAL REVIEW) CHEM. SOC. REV., 2010, **39**, 228-240.
- [19]. Yifei Wang, Dennis Y.C. Leung, Jin Xuan, Huizhi Wang. A review on unitized regenerative fuel cell technologies, part B: Unitized regenerative alkaline fuel cell, solid oxide fuel cell, and microfluidic fuel cell. *Renewable and Sustainable Energy Reviews* Volume 75, August 2017, Pages 775-795. <https://doi.org/10.1016/j.rser.2016.11.054>.
- [20]. Yong Li, Jian Song, Jie Yang. Graphene models and nano-scale characterization technologies for fuel cell vehicle electrodes. *Renewable and Sustainable Energy Reviews*. Volume 42, February 2015, Pages 66-77. <https://doi.org/10.1016/j.rser.2014.10.005>
- [21]. Bidyut Paul, John Andrews. PEM unitised reversible/regenerative hydrogen fuel cell systems: State of the art and technical challenges. *Renewable and Sustainable Energy Reviews*. Volume 79, November 2017, Pages 585-599. <https://doi.org/10.1016/j.rser.2017.05.112>
- [22]. Agnieszka Iwan, Marek Malinowski, Grzegorz, Pasciak. Polymer fuel cell components modified by graphene: Electrodes, electrolytes and bipolar plates. *Renewable and Sustainable Energy Reviews* Volume 49, September 2015, Pages 954-967. <https://doi.org/10.1016/j.rser.2015.04.093>.
- [23]. Chun Yik Wong, Wai Yin Wong, Kee Shyuan Loh, Abu Bakar Mohamad. Study of the plasticising effect on polymer and its development in fuel cell application. *Renewable and Sustainable Energy Reviews*. Volume 79, November 2017, Pages 794-805. <https://doi.org/10.1016/j.rser.2017.05.154>.
- [24]. Sergio Yesid Gómez Dachamir Hotza. Current developments in reversible solid oxide fuel cells. *Renewable and Sustainable Energy Reviews*. Volume 61, August 2016, Pages 155-174. <https://doi.org/10.1016/j.rser.2016.03.005>.
- [25]. Nikdalila Radenahmad, Ahmed Afif, Pg Iskandar Petra, Seikh M.H.Rahman, Sten-G.Eriksson, Abul K.Azad. Proton-conducting electrolytes for direct methanol and direct urea fuel cells – A state-of-the-art review. *Renewable and Sustainable Energy Reviews*. Volume 57, May 2016, Pages 1347-1358. <https://doi.org/10.1016/j.rser.2015.12.103>.

- [26]. Ahmed, ElMekawy, Hanaa M.Hegab, Dusan Losic, Christopher P.Saint, Deepak Pant. Applications of graphene in microbial fuel cells: The gap between promise and reality. *Renewable and Sustainable Energy Reviews*. Volume 72, May 2017, Pages 1389-1403. <https://doi.org/10.1016/j.rser.2016.10.044>.
- [27]. Theo Elmer, Mark Worall, Shenyi Wu, Saffa B. Riffat. Fuel cell technology for domestic built environment applications: State of-the-art review. *Renewable and Sustainable Energy Reviews* Volume 42, February 2015, Pages 913-931. <https://doi.org/10.1016/j.rser.2014.10.080>.
- [28]. Vipin Das, Sanjeevikumar Padmanaban, Karthikeyan Venkitesamy, Rajasekar Selvamuthu kumaran, Frede Blaabjerg, Pierluigi Siano. Recent advances and challenges of fuel cell based power system architectures and control – A review. *Renewable and Sustainable Energy Reviews*. Volume 73, June 2017, Pages 10-18. <https://doi.org/10.1016/j.rser.2017.01.148>.
- [29]. Seema S.Munjewar, Shashikant B.Thombre Ranjan K.Mallick. Approaches to overcome the barrier issues of passive direct methanol fuel cell – Review. *Renewable and Sustainable Energy Reviews* Volume 67, January 2017, Pages 1087-1104. <https://doi.org/10.1016/j.rser.2016.09.002>.
- [30]. C.Y.Park T.H.Lee, S.E.Dorris, U.Balachandran. Hydrogen production from fossil and renewable sources using an oxygen transport membrane. *International Journal of Hydrogen Energy* Volume 35, Issue 9, May 2010, Pages 4103-4110. <https://doi.org/10.1016/j.ijhydene.2010.02.025>
- [31]. Kai Feng, Zhuguo Li, Xun Cai, Paul K.Chu. Corrosion behavior and electrical conductivity of niobium implanted 316L stainless steel used as bipolar plates in polymer electrolyte membrane fuel cells. *Surface and Coatings Technology*. Volume 205, Issue 1, 25 September 2010, Pages 85-91. <https://doi.org/10.1016/j.surfcoat.2010.06.009>
- [32]. R. Taherian, Manufacture, test, modeling of polymer-based nanocomposite utilized in bipolar plate of PEM fuel cell, in: *Material Engineering*, Shiraz University, 2012, p. 246.
- [33]. R. Taherian. A review of composite and metallic bipolar plates in proton exchange membrane fuel cell: Materials, fabrication, and material selection. *Journal of Power Sources* 265 (2014) 370-390. <https://doi.org/10.1016/j.jpowsour.2014.04.081>

- [34]. Kai Feng, Yao Shen, Hailin Sun, Dongan Liu, Quanzhang An, Xun Cai, Paul K.Chu. Conductive amorphous carbon-coated 316L stainless steel as bipolar plates in polymer electrolyte membrane fuel cells. *International Journal of Hydrogen Energy* Volume 34, Issue 16, August 2009, Pages 6771-6777. <https://doi.org/10.1016/j.ijhydene.2009.06.030>.
- [35]. Moucheng Li, Suzhen Luo, Chaoliu Zeng, Jianian Shen, Haichao Lin, Chu'nan Cao. Corrosion behavior of TiN coated type 316 stainless steel in simulated PEMFC environments. *Corrosion Science*. Volume 46, Issue 6, June 2004, Pages 1369-1380. [https://doi.org/10.1016/S0010-938X\(03\)00187-2](https://doi.org/10.1016/S0010-938X(03)00187-2)
- [36]. Collier A., Wang H., Yuan X.Z., Zhang J., Wilkinson D.P. Degradation of polymer electrolyte membranes. *Int. J. Hydrog. Energy*. 2006;31:1838–1854. doi: 10.1016/j.ijhydene.2006.05.006.
- [37]. Michael J. Kelly, Bernhard Egger, Günter Fafilek, Jürgen O.B esenhard, Hermann Kronberger, Gerhard E.Nauer. Conductivity of polymer electrolyte membranes by impedance spectroscopy with microelectrodes. *Solid State Ionics*. Volume 176, Issues 25–28, 15 August 2005, Pages 2111-2114. <https://doi.org/10.1016/j.ssi.2004.07.071>
- [38]. Michael J.Kelly, Günter Fafilek, Jürgen O. Besenhard, Hermann Kronberger, Gerhard E.Nauer. Contaminant absorption and conductivity in polymer electrolyte membranes. *Journal of Power Sources* Volume 145, Issue 2, 18 August 2005, Pages 249-252. <https://doi.org/10.1016/j.jpowsour.2005.01.064>
- [39]. T. Okada, Effect of ionic contaminants, in: W. Vielstich, H.A. Gasteiger, A. Lamm (Eds.), *Handbook of Fuel Cells Fundamentals, Technology and Applications* vol. 3, John Wiley and Sons, Ltd., 2003, p. 627.
- [40]. Minglian Shi, Fred C.Anson. Dehydration of protonated Nafion® coatings induced by cation exchange and monitored by quartz crystal microgravimetry. *Journal of Electroanalytical Chemistry*. Volume 425, Issues 1–2, 30 March 1997, Pages 117-123. [https://doi.org/10.1016/S0022-0728\(96\)04945-5](https://doi.org/10.1016/S0022-0728(96)04945-5).
- [41]. M.P.Brady, M. Abd Elhamid, G.Dadheech, J. Bradley, T.J.Toops, H.M.MeyerIII, P.F.Tortorelli. Manufacturing and performance assessment of stamped, laser welded, and nitrided FeCrV stainless steel bipolar plates for proton exchange membrane fuel cells. *Int. J. Hydrogen Energy* 38 (2013) 4734-4739. <https://doi.org/10.1016/j.ijhydene.2013.01.143>.

[42]. M. P. Brady, B. Yang, K. L. More, P. F. Tortorelli, Tim Armstrong, H. Wang, J. A. Turner. Cost-Effective Surface Modification For Metallic Bipolar Plates, Oak ridge National Laboratory, 2005. Fuel Cell Tech Team Meeting, USCAR facility, Southfield, MI, January 18, 2006.

[43]. Claudio Mele, Benedetto Bozzini. Localised corrosion processes of austenitic stainless steel bipolar plates for polymer electrolyte membrane fuel cells. *Journal of Power Sources* Volume 195, Issue 11, 1 June 2010, Pages 3590-3596. <https://doi.org/10.1016/j.jpowsour.2009.11.144>

[44]. M.P.Brady, H.Wang, J.A.Turner, H.M.MeyerIII, K.L.More, P.F.Tortorelli, B.D.McCarthy. Pre-oxidized and nitrated stainless steel alloy foil for proton exchange membrane fuel cell bipolar plates: Part 1. Corrosion, interfacial contact resistance, and surface structure. *Journal of Power Sources*. Volume 195, Issue 17, 1 September 2010, Pages 5610-5618. <https://doi.org/10.1016/j.jpowsour.2010.03.055>.

[45]. Todd J.Toops, Michael P.Brady, Peter F.Tortorelli, Josh A.Pihl, Francisco Estevez, DanielConnors, Fernando Garzon, Tommy Rockward, Don Gervasio, William Mylan, Sree Harsha Kosaraju. Pre-oxidized and nitrated stainless steel alloy foil for proton exchange membrane fuel cell bipolar plates. Part 2: Single-cell fuel cell evaluation of stamped plates. *Journal of Power Sources*. Volume 195, Issue 17, 1 September 2010, Pages 5619-5627. <https://doi.org/10.1016/j.jpowsour.2010.03.056>

[46]. P. Chatterjee, V. M. Athawale, and S. Chakraborty, Materials selection using complex proportional assessment and evaluation of mixed data methods, *Mater. Des.*, vol. 32, no. 2, pp. 851–860, 2011.

[47]. Isa Bar-On, Randy Kirchain, Richard Roth. Technical cost analysis for PEM fuel cells. *Journal of Power Sources*. Volume 109, Issue 1, 15 June 2002, Pages 71-75. [https://doi.org/10.1016/S0378-7753\(02\)00062-9](https://doi.org/10.1016/S0378-7753(02)00062-9).

[48]. K.Jayakumar, S. Pandiyan, N.Rajalakshmi, K.S.Dhathathreyan. Cost-benefit analysis of commercial bipolar plates for PEMFC's. *Journal of Power Sources*. Volume 161, Issue 1, 20 October 2006, Pages 454-459. <https://doi.org/10.1016/j.jpowsour.2006.04.128>.

[49]. A.Jahan, M.Y.Ismail, S.M.Sapuan, F.Mustapha. Material screening and choosing methods – A review. *Materials & Design* Volume 31, Issue 2, February 2010, Pages 696-705. <https://doi.org/10.1016/j.matdes.2009.08.013>.

[50]. A.Shanian, O.Savadogo. TOPSIS multiple-criteria decision support analysis for material selection of metallic bipolar plates for polymer electrolyte fuel cell. *Journal of Power Sources*. Volume 159, Issue 2, 22 September 2006, Pages 1095-1104. <https://doi.org/10.1016/j.jpowsour.2005.12.092>.

[51]. S. Radhakrishnan, Developments in conducting polymer composites and coatings for bipolar plates, in: Reports for NCL, 2012.copper

[52]. José Barranco, Félix Barreras, Antonio Lozano, Mario Maza. Influence of CrN-coating thickness on the corrosion resistance behaviour of aluminium-based bipolar plates. *Journal of Power Sources*. Volume 196, Issue 9, 1 May 2011, Pages 4283-4289. <https://doi.org/10.1016/j.jpowsour.2010.11.069>.

[53]. A.Pozio, F.Zaza, A.Masci, R.F.Silva. Bipolar plate materials for PEMFCs: A conductivity and stability study. *Journal of Power Sources* Volume 179, Issue 2, 1 May 2008, Pages 631-639. <https://doi.org/10.1016/j.jpowsour.2008.01.038>

[54]. Shen Chunhui, Pan Mu, Yuan Qin, Yuan Runzhang. Studies on Preparation and Performance of Sodium Silicate/Graphite Conductive Composites. First Published May 1, 2006. *Journal of Composite materials*. <https://doi.org/10.1177/0021998306061296>

[55]. Bing Luo, Mingruo Hu, Fei Li, Guangyi Cao. A novel material fabrication method for the PEM fuel cell bipolar plate. *International Journal of Hydrogen Energy*. Volume 35, Issue 7, April 2010, Pages 2643-2647. <https://doi.org/10.1016/j.ijhydene.2009.04.030>

[56]. Zhu Bin, Mei Bingchu, Shen Chunhui, Yuan Runzhang. Study on the electrical and mechanical properties of polyvinylidene fluoride/titanium silicon carbide composite bipolar plates. *Journal of Power Sources*. Volume 161, Issue 2, 27 October 2006, Pages 997-1001. <https://doi.org/10.1016/j.jpowsour.2006.05.024>

[57]. Man Wu, Leon L.Shaw. A novel concept of carbon-filled polymer blends for applications in PEM fuel cell bipolar plates. *International Journal of Hydrogen Energy*. Volume 30, Issue 4, March 2005, Pages 373-380. <https://doi.org/10.1016/j.ijhydene.2004.08.005>.

[58]. Shigehiro Kitta, Hiroyuki Uchida, Masahiro Watanabe. Metal separators coated with carbon/resin composite layers for PEFCs. *Electrochimica Acta*. Volume 53, Issue 4, 31 December 2007, Pages 2025-2033.

[59]. S.R.Dhakate, S.Sharma, M.Borah, R.B.Mathur, T.L.Dham. Expanded graphite-based electrically conductive composites as bipolar plate for PEM fuel cell. *International Journal of Hydrogen Energy*. Volume 33, Issue 23, December 2008, Pages 7146-7152. <https://doi.org/10.1016/j.ijhydene.2008.09.004>

[60]. Rungsima Yeetsorn, Michael Fowler, Costas Tzoganakis, Wang Yuhua, and Mali Taylor, Polypropylene composites for polymer electrolyte membrane fuel cell bipolar plates, *Macromolecular Symposia* 264 (2008), no. 1, 34-43.

[61]. J. Zhang, Y.W. Zou, J. He, J. Influence of graphite particle size and its shape on performance of carbon composite bipolar plate. *Journal of Zhejiang University Science*. ISSN 1009-3095. <http://www.zju.edu.cn/jzus>. Sci. 6A (10) (2005) 1080-1083.

[62]. D. P. Davies, P. L. Adcock, M. Turpin, and S. J. Rowen, "Bipolar plate materials for solid polymer fuel cells," *Journal of Applied Electrochemistry*, vol. 30, no. 1, pp. 101–105, 2000. <https://doi.org/10.1023/A:1003831406406>. ISSN: 1572-8838.

[63]. Jayaraj J, Kim YC, Seok HK, Kim KB, Fleury E. Development of metallic glasses for bipolar plate application. *Materials Science and Engineering: A*. 2007;449-451:30-33.

[64]. Yu Fu, Guoqiang Lin, Ming Hou, Bo Wu, Hongkai Li, Lixing Hao, Zhigang Shao, Baolian Yi. Optimized Cr-nitride film on 316L stainless steel as proton exchange membrane fuel cell bipolar plate. *International Journal of Hydrogen Energy*. Volume 34, Issue 1, January 2009, Pages 453-458. <https://doi.org/10.1016/j.ijhydene.2008.09.104>.

[65]. R. Tian. Chromium nitride/Cr coated 316L stainless steel as bipolar plate for proton exchange membrane fuel cell. *Journal of Power Sources*. Volume 196, Issue 3, 1 February 2011, Pages 1258-1263. <https://doi.org/10.1016/j.jpowsour.2010.08.028>.

[66]. Byung-Chu Cha, Yong-Zoo You, Sung-Tae Hong, Jun-Ho Kim, Dae-Wook Kim, Byung-Seok Lee, Sun-Kwang Kim. Nitride films as protective layers for metallic bipolar plates of polymer electrolyte membrane fuel cell stacks. *International Journal of Hydrogen Energy* Volume 36, Issue 7, April 2011, Pages 4565-4572.



[67]. Dongming Zhang, Lu Guo, Liangtao Duan, Wei-HsingTuan. Preparation of Cr-based multilayer coating on stainless steel as bipolar plate for PEMFCs by magnetron sputtering. *International Journal of Hydrogen Energy*. Volume 36, Issue 3, February 2011, Pages 2184-2189. <https://doi.org/10.1016/j.ijhydene.2010.10.085>.

[68]. Min Zhang, Bo Wu, Guoqiang Lin, Zhigang Shao, Ming Hou, BaolianYi. Arc ion plated Cr/CrN/Cr multilayers on 316L stainless steel as bipolar plates for polymer electrolyte membrane fuel cells. *Journal of Power Sources*. Volume 196, Issue 6, 15 March 2011, Pages 3249-3254. <https://doi.org/10.1016/j.jpowsour.2010.11.154>

[69]. D.-H. Han, W.-H.Hong, H.S.Choi, J.J.Lee. Inductively coupled plasma nitriding of chromium electroplated AISI 316L stainless steel for PEMFC bipolar plate. *International Journal of Hydrogen Energy*. Volume 34, Issue 5, March 2009, Pages 2387-2395. <https://doi.org/10.1016/j.ijhydene.2009.01.004>

[70]. W.G.Lee, K.H.Cho, S.B.Lee, S.B.Park, H.Jang. Electrochemical response of zirconia-coated 316L stainless-steel in a simulated proton exchange membrane fuel cell environment. *Journal of Alloys and Compounds*. Volume 474, Issues 1–2, 17 April 2009, Pages 268-272. <https://doi.org/10.1016/j.jallcom.2008.06.093>.

[71]. Yu Fu, Guoqiang Lin, Ming Hou, Bo Wu, Zhigang Shao, Baolian Yi. Carbon-based films coated 316L stainless steel as bipolar plate for proton exchange membrane fuel cells. *International Journal of Hydrogen Energy*. Volume 34, Issue 1, January 2009, Pages 405-409. <https://doi.org/10.1016/j.ijhydene.2008.10.068>.

[72]. Seung-Taek Myung, Masanobu Kumagai, Ryo Asaishi, Yang-Kook Sun, Hitoshi Yashiro. Nanoparticle TiN-coated type 310S stainless steel as bipolar plates for polymer electrolyte membrane fuel cell. *Electrochemistry Communications*. Volume 10, Issue 3, March 2008, Pages 480-484.

[73]. Heli Wang, John A.Turner, Xiaonan Li, Glenn Teeter. Process modification for coating SnO<sub>2</sub>:F on stainless steels for PEM fuel cell bipolar plates. *Journal of Power Sources*. Volume 178, Issue 1, 15 March 2008, Pages 238-247. <https://doi.org/10.1016/j.jpowsour.2007.12.010>

[74]. P.F. Ju, Y. Zuo, Y.M. Tang, X.H. Zhao, The enhanced passivation of 316 L stainless steel in a simulated fuel cell environmental by surface plating with palladium, *Corros. Sci.* 66 (2013) 330–336.

- [75]. Ching-Yuan Bai, Ming-Der Ger, Min-Sheng Wu. Corrosion behaviors and contact resistances of the low-carbon steel bipolar plate with a chromized coating containing carbides and nitrides. *International Journal of Hydrogen Energy*. Volume 34, Issue 16, August 2009, Pages 6778-6789. <https://doi.org/10.1016/j.ijhydene.2009.05.103>.
- [76]. Dearnaley G. Ion implantation and ion assisted coatings for wear resistance in metals. *Surf Eng* 1986;2(3):213-22. <https://doi.org/10.1179/sur.1986.2.3.213>.
- [77]. Husby H. Carbon based coatings for metallic bipolar plates in PEM fuel cells. 2013. Norwegian University of Science and Technology. Department of Materials Science and Engineering.
- [78]. G. Susanna, L. Salamandra, T. M. Brown, A. Di Carlo, F. Brunetti, and A. Reale, "Airbrush spray-coating of polymer bulk-heterojunction solar cells," *Solar Energy Materials and Solar Cells*, vol. 95, no. 7, pp. 1775–1778, 2011.
- [79]. Gago A, Ansar A, Wagner N, Arnold J, Friedrich KA. Titanium coatings deposited by thermal spraying for bipolar plates of PEM electrolyzers. In: 4th European PEFC and H2 forum 2-5 July 2013, Lucerne Switzerland; 2013.
- [80]. Pawlowski L. The science and engineering of thermal spray coatings. John Wiley & Sons; 2008. ISB: 978 – 0 – 471 – 49049 – 4. <https://doi.org/10.1002/9780470754085.ch8>
- [81]. Meng-Yu Tsai, Chin-Chi Hsu, Ping-Hei Chen, Chao-Sung Lin, Alexander Chen. Surface modification on a glass surface with a combination technique of sol–gel and air brushing processes. *Applied Surface Science*. Volume 257, Issue 20, 1 August 2011, Pages 8640-8646. <https://doi.org/10.1016/j.apsusc.2011.05.041>
- [82]. Bratean L. Thermal spraying arc process with two dissimilar wires equality tests. *Procedia - Social and Behavioral Sciences*. Volume 180, 5 May 2015, Pages 1116-1121. <https://doi.org/10.1016/j.sbspro.2015.02.222>.
- [83]. La Notte L, Salamandra L, Zampetti A, Brunetti F, Brown TM, Di Carlo A, et al. Airbrush spray coating of amorphous titanium dioxide for inverted polymer solar cells. *Int J Photoenergy* 2012;2012. <http://dx.doi.org/10.1155/2012/897595>
- [84]. Sun H, Cooke K, Eitzinger G, Hamilton P, Pollet B. Development of PVD coatings for PEMFC metallic bipolar plates. *Thin Solid Films*. Volume 528, 15 January 2013, Pages 199-204. <https://doi.org/10.1016/j.tsf.2012.10.094>

- [85]. Liu X, Kavanagh J, Matthews A, Leyland A. The combined effects of Cu and Ag on the nanostructure and mechanical properties of CrCuAgN PVD coatings. *Surf Coatings Technol* 2015;284:101-11.
- [86]. Lee S, Nam K, Hong S, Lee J. Low temperature deposition of TiB<sub>2</sub> by inductively coupled plasma assisted CVD. *Surf Coatings Technol* 2007;201:5211-5
- [87]. Dong H, Qi P-Y, Li X, Llewellyn R. Improving the erosion - corrosion resistance of AISI 316 austenitic stainless steel by low-temperature plasma surface alloying with N and C. *Mater Sci Eng A* 2006;431:137-45.
- [88]. Liu R, Li X, Hu X, Dong H. Surface modification of a medical grade Co-Cr-Mo alloy by low-temperature plasma surface alloying with nitrogen and carbon. *Surf Coat Technol* 2013;232:906-11.
- [89]. Lin K, Li X, Tian L, Dong H. Active screen plasma surface co-alloying of 316 austenitic stainless steel with both nitrogen and niobium for the application of bipolar plates in proton exchange membrane fuel cells. *Int J Hydrogen Energy* 2015;40:10281-92.
- [90]. Zhang M, Lin G, Wu B, Shao Z. Composition optimization of arc ion plated CrN<sub>x</sub> films on 316L stainless steel as bipolar plates for polymer electrolyte membrane fuel cells. *J Power Sources* 2012;205:318-23.
- [91]. Zhang M, Hu L, Lin G, Shao Z. Honeycomb-like nanocomposite Ti-Ag-N films prepared by pulsed bias arc ion plating on titanium as bipolar plates for unitized regenerative fuel cells. *Journal of Power Sources*. Volume 198, 15 January 2012, Pages 196-202. <https://doi.org/10.1016/j.jpowsour.2011.10.022>
- [92]. Shreir LL. *Corrosion: corrosion control*. Newnes; 2013. ISBN: 1483164128, 9781483164120
- [93]. Antonucci P, Romeo F, Minutoli M, Alderucci E, Giordano N. Electrochemical corrosion behavior of carbon black in phosphoric acid. *Carbon*. Volume 26, Issue 2, 1988, Pages 197-203. [https://doi.org/10.1016/0008-6223\(88\)90037-1](https://doi.org/10.1016/0008-6223(88)90037-1)
- [94]. Singh H, Puri D, Prakash S. An overview of Na<sub>2</sub>SO<sub>4</sub> and/or V<sub>2</sub>O<sub>5</sub> induced hot corrosion of Fe-and Ni-based super alloys. *Reviews on advanced materials science* 16(1):27-50
- [95]. Ofstad A, Davey J, Sunde S, Borup RL. Carbon corrosion of a PEMFC during shut-down/start-up when using an air purge procedure. *ECS Trans* 2008;16:1301-11.

[96]. Melchers RE. Corrosion uncertainty modelling for steel structures. Journal of Constructional Steel Research, Volume 52, 3-19.

[97]. Vaysburd A, Emmons P. How to make today's repairs durable for tomorrow - corrosion protection in concrete repair. Constr Build Mater 2000;14:189-97.

[98]. Melchers RE. The effect of corrosion on the structural reliability of steel offshore structures. Corros Sci 2005;47:2391-410.

[99]. Kongstein OE, CEA NG, Ødegaard A. «NEXPEL Project» Next generation PEM electrolyzer for sustainable hydrogen production WP5 “Porous current collectors and materials for bipolar plate” [Bibliographic review].

[100]. Zhang L, Finch J, Gontarz G, Wang C. Development of low cost PEMFC metal bipolar plate. ECS Trans 2010;33:955-61.

[101]. FUJII H, MAEDA T. Titanium alloys developed by Nippon steel & Sumitomo metal corporation. Nippon Steel & Sumitomo Metal Tech Rep 2014;106:16-21.